



Rodrigues, P. G., Martinelli, A. G., Schultz, C. L., Corfe, I. J., Gill, P. G., Soares, M. B., & Rayfield, E. J. (2018). Digital cranial endocast of *Riograndia guaibensis* (Late Triassic, Brazil) sheds light on the evolution of the brain in non-mammalian cynodonts. *Historical Biology*. Advance online publication.  
<https://doi.org/10.1080/08912963.2018.1427742>

Peer reviewed version

Link to published version (if available):  
[10.1080/08912963.2018.1427742](https://doi.org/10.1080/08912963.2018.1427742)

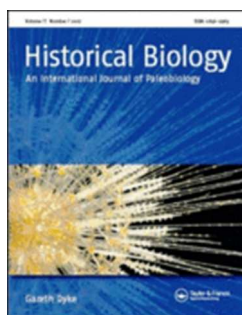
[Link to publication record on the Bristol Research Portal](#)  
PDF-document

This is the author accepted manuscript (AAM). The final published version (version of record) is available online via Taylor & Francis at <https://www.tandfonline.com/doi/full/10.1080/08912963.2018.1427742?scroll=top&needAccess=true>. Please refer to any applicable terms of use of the publisher.

## University of Bristol – Bristol Research Portal

### General rights

This document is made available in accordance with publisher policies. Please cite only the published version using the reference above. Full terms of use are available: <http://www.bristol.ac.uk/red/research-policy/pure/user-guides/brp-terms/>



**Digital endocast of *Riograndia guaibensis* (Late Triassic, Brazil) and the evolution of the brain in non-mammalian cynodonts.**

|                               |   |
|-------------------------------|---|
| Journal:                      | <i>Historical Biology</i>   |
| Manuscript ID                 | GHBI-2017-0104  |
| Manuscript Type:              | Original Article  |
| Date Submitted by the Author: | 26-May-2017   |
| Complete List of Authors:     | Rodrigues, Pablo; Universidade Federal do Rio Grande do Sul, Departamento de Paleontologia e Estratigrafia<br>Martinelli, AGustin; Universidade Federal de Rio Grande do Sul, Departamento de Paleontologia e Estratigrafia<br>Schultz, Cesar; Universidade Federal do Rio Grande do Sul, Departamento de Paleontologia e Estratigrafia<br>Corfe, Ian; University of Helsinki, Jernvall EvoDevo Lab, Institute of Biotechnology.<br>Gill, Pam; University of Bristol, School of Earth Sciences<br>Rayfield, E; University of Bristol, School of Earth Sciences<br>Soares, Marina ; Universidade Federal do Rio Grande do Sul, Departamento de Paleontologia e Estratigrafia |
| Keywords:                     | Mammalian brain evolution, Endocast, Riograndia, Cynodonts, $\mu$ CT scan, Triassic   |
|                               |   |

SCHOLARONE™  
Manuscripts

## Digital endocast of *Riograndia guaibensis* (Late Triassic, Brazil) and the evolution of the brain in non-mammalian cynodonts.

Pablo Gusmão Rodrigues<sup>1</sup>; Agustín G. Martinelli<sup>1</sup>; Cesar Leandro Schultz<sup>1</sup>; Ian J. Corfe<sup>2</sup>; Pamela G. Gill<sup>3</sup>; Emily J. Rayfield<sup>3</sup>; Marina B. Soares<sup>1</sup>

<sup>1</sup>Departamento de Paleontologia e Biostratigrafia, Instituto de Geociências, Universidade Federal do Rio Grande do Sul, Porto Alegre, RS; <sup>2</sup>Jernvall EvoDevo Lab, Institute of Biotechnology, University of Helsinki, Helsinki, Finland; <sup>3</sup>School of Earth Sciences, University of Bristol, Bristol, UK. <sup>4</sup>Department of Physics, University of Helsinki, Helsinki, Finland.

### Abstract

A digital cranial endocast of the specimen UFRGS-PV-596-T, *Riograndia guaibensis*, was obtained from  $\mu$ CT scan images. This is a small cynodont, closely related to mammaliaforms, from the Late Triassic of Brazil. *Riograndia* presents big olfactory bulb casts and the cerebral hemispheres region is relatively wider than in other non-mammaliaform cynodonts. Impressions of vessels were observed and a conspicuous mark on the dorsal surface was interpreted as the transverse sinus. The encephalization quotient calculated is greater than the range of the most non-mammaliaform cynodonts. The ratios between linear and area measurements of the dorsal surface suggests four evolutionary changes from a basal eucynodont morphology to mammaliaformes, evolving the increase of the relative size of the olfactory bulbs and the width of the cerebral hemispheres and cerebellum. The data supports the hypothesis of the neurological evolution of the mammalian lineage starting by a trend of the increase of the olfactory bulbs, which is associated to adaptations on the nasal cavity. This trend must be linked to the selective pressures for the small faunivorous, and probably nocturnal, animals, and represents an initial improvement of the sensory receptor system, leading to further development of the “superior” structures for sensorial processing and integration.

**Keywords** Mammalian brain evolution; Endocast; *Riograndia*; Cynodonts;  $\mu$ CT scan; Triassic

### INTRODUCTION

Cranial endocasts are important tools to study the brain of some extinct taxa, and so, to make inferences about the behavior, sensorial acuity, and motor control in extinct animals. Moreover, within non-mammalian cynodonts, these paleoneurological studies can help to understand the evolutionary changes along the mammalian lineage, since living mammals are distinguished by relatively larger and more complex brains than other vertebrates (Kielan-Jaworowska et al. 2004; Kemp 2009). Although the intracranial space is occupied also for meninges and blood vessels, cranial endocasts

1  
2  
3 show neuroanatomical external structures, especially in mammals and birds, because,  
4 contrary to small-brained non-mammalian and non-avian tetrapods, their brains largely  
5 fill the endocranial space (Jerison 1973; Starck 1979). For non-mammaliaform  
6 cynodonts, Kemp (2009) raised the possibility that their endocasts do not represent the  
7 actual shape of the brain, but in any case, some important features have been reported  
8 from some taxa as: the Early Triassic *Nyctosaurus larvatus* (= *Thrinaxodon liorhinus*)  
9 and *Diademodon* (Watson 1913), the Late Triassic *Exaeretodon* (Bonaparte 1966), the  
10 Early Triassic *Trirachodon* (Hopson 1979), the Late Permian *Procynosuchus* (Kemp  
11 1979), the Middle Triassic *Massetognathus*, *Probelesodon* (Quiroga 1979, 1980a,  
12 synonymized to *Chiniquodon*, Abdala & Giannini, 2002) and *Probainognathus*  
13 (Quiroga 1980b, c), as well as the Late Triassic *Therioherpeton* (Quiroga 1984) and  
14 *Brasilitherium* (Rodrigues et al. 2013).  
15  
16  
17  
18  
19  
20  
21  
22  
23

#### 24 **Common features observed in endocasts of non-mammaliaform cynodonts**

25  
26 In general, the basic design of the endocast of non-mammaliaform cynodonts  
27 point to a narrow brain and commonly with tubular cerebral hemispheres, although  
28 Kemp (2009) have appointed that the region of the cerebral hemispheres could have  
29 been substantially deeper than wide, since in that region of the skull there is no bony  
30 floor for the brain cavity. The main structures usually visible in these endocasts are  
31 well-defined olfactory bulb casts and the cerebellar region, whose lateral extension is  
32 indicated by prominent paraflocculi, which fill the subarcuate fossa on the  
33 supraoccipital and periotic components of the braincase (Kemp, 2009). Moreover, in  
34 ventral view is common the identification of the hypophyseal cast, which fills the sella  
35 turcica on the basisphenoid/parasphenoid. Another structure which can be observed in  
36 non-mammalian cynodont endocasts is the vermis on the dorsal surface of the cerebellar  
37 region, indicated by Kielan-Jaworowska *et al.* (2004) for the eucynodont *Thrinaxodon*,  
38 although it is not reported in other descriptions (Watson 1913; Hopson 1979; Quiroga  
39 1979, 1980a, b, 1984) and there is the suggestion that the dorsal depression between the  
40 parietal and interparietal bones is filled indeed by the superior sagittal sinus (Rowe et al.  
41 1995; Kemp 2009). Also controversial is the dorsal exposure of the midbrain coliculli,  
42 reported by Quiroga (1980b, c) for *Probainognathus*, while Kielan-Jaworowska et al.  
43 (2004) warn about the possibility of marks of post-mortem changes in parts of the brain  
44 and meninges on taxa with endocasts without a clear definition of the transverse sinus  
45 marking the posterior limit of the cerebral hemispheres. Furthermore, Macrini et al.  
46  
47  
48  
49  
50  
51  
52  
53  
54  
55  
56  
57  
58  
59  
60

(2007b) claimed that the non-exposure of the midbrain should be the plesiomorphic condition for the mammalian crown-group.

### Quantitative/volumetric approaches

The Encephalization Quotient (EQ) is the most widely used measure for comparison of different taxa relative to brain size, including non-mammalian cynodonts and extinct mammals (e.g. Quiroga, 1979, 1980a, b, Kielan-Jaworowska 1983, 1984; Kielan-Jaworowska and Lancaster 2004; Macrini et al. 2007b; Rowe et al. 2011; Rodrigues et al. 2013). The EQ, as developed by Jerison (1973) and discussed by Eisenberg (1981), consists of a ratio between the volume of the brain weight of an animal and the brain weight expected for an animal of the same mass, based on allometric regressions for the ratio brain weight/body weight, empirically verified for different taxa of a group defined as parameter. The use of EQs, however, has already been the target of criticism associated mainly to the significance of the relative brain size as an indicator of the capacity to integrate information (Butler and Hodos 1996). In addition, there are methodological difficulties, specially for the study of fossils, since the body mass must be estimated (from different parameters in the fossils as skull length, postcanine teeth, lengths of long bones, mid-shaft circumferences of long bones, cross-sectional area of vertebrae, etc.), and the endocast volume (assuming that 1 cm<sup>3</sup> is equivalent to 1 g) cannot correspond to the actual volume occupied by the brain in the endocranial cavity (Rodrigues et al., 2013). Even so, the values of EQ from former studies with non-mammalian cynodonts indicate, in general, an increased brain volume in relation to the estimated body mass in taxa successively more closely related to mammals, but it is not so clear within non-mammaliaform cynodonts: *Thrinaxodon*, 0.10 (Jerison, 1973); *Diademodon*, 0.14 (Quiroga 1980b), and 0.21 (Jerison 1973); *Massetognathus*, 0.15 and 0.22 (Quiroga 1979, 1980b); *Exaeretodon*, 0.10 and 0.15 (Quiroga 1980b), *Probelesodon*, 0.13 and 0.18 (Quiroga 1979, 1980b); *Probainognathus*, 0.12 and 0.17 (Quiroga 1980a, b); *Brasilitherium*, 0.15 and 0.22 (Rodrigues et al, 2013); *Morganucodon*, 0.32 (Rowe et al. 2011); *Hadrocodium*, 0.49 (Rowe et al. 2011); living monotremes 0.75 to 0.89 (Macrini et al. 2007a); *Triconodon*, 0.49 (Kielan-Jaworowska 1983). Regarding to the EQs of non-mammaliaform cynodonts, Rodrigues et al. (2013) suggested that the values may be higher than they should due to the equation used to estimate the body mass (in turn, then overestimated).

### The evolution of the mammalian brain among non-mammalian cynodonts

In addition to a tendency to increase in overall size, the brain evolution towards mammals presents changes in different anatomical features, whose variation can also be observed in relation to the whole endocast or the skull size. Thus, in an evolutionary sequence towards the mammalian brain, the first clear change observed from the endocasts of the non-mammaliaform cynodonts is the loss of the parietal eye (and perhaps the whole parietal-pineal complex) in most group Eucynodontia, although some eucynodonts taxa, such as *Diademodon*, *Trirachodon* and *Massetognathus*, present the primitive state (e.g., Quiroga, 1979; Hopson and Kitching 2001). Moreover, the division between the cerebral hemisphere casts by a median sulcus seems to be more defined in *Probainognathus* (Quiroga 1980a, b) than in the taxa *Thrinaxodon* (Kielan-Jaworowska et al. 2004), *Exaeretodon* (Bonaparte 1966), *Massetognathus* and *Probeleson* (*Chiniquodon*) (Quiroga 1979). Associated to this feature, the cerebral hemisphere region becomes wider, mainly near to their posterior limit in *Probainognathus* and taxa more closely related to mammals. *Brasilitherium* also presents a clear median sulcus in the cerebral hemispheres region, suggesting a phylogenetic significance, since this taxon is more nearly related to mammaliaforms than the others quoted above. Rodrigues et al. (2013), also reported for *Brasilitherium* the relative size of the olfactory bulb casts larger than in other taxa of non-mammaliaform cynodonts as well as mammaliaforms and suggesting a trend of increase of relative size olfactory bulbs among non-mammaliaform cynodonts successively more related to mammals.

Among non-mammalian mammaliaforms, Luo et al. (2001) reported a progressive increase of the width of the posterior (cerebellar) region in *Sinoconodon*, *Haldanodon*, *Morganucodon*, and *Hadrocodium*, and an increase of width of the cerebral hemisphere region is also highlighted for these two last taxa in the summarization of Kielan-Jaworowska et al. (2004). These authors also indicate in the endocast of *Morganucodon* the cerebral hemisphere region relatively wider compared to non-mammaliaform cynodonts and *Sinoconodon* (in which the parietal bones are subvertically disposed, having less endocranial space in this region). Besides, they evinced the presence of marks interpreted as transversal gyres at the dorsal surface of the cerebellum cast, and, and the division of the dorsal surface in two hemispheres. Furthermore, the division of the cerebral and cerebellar cavities in *Morganucodon*, by an ossified septum, i.e., the tentorium (tentorium osseum), was suggested by Kermack et al. (1981) but this suggestion is controversial (e.g., Kielan-Jaworowska 1997).

1  
2  
3 Kemp (2009), suggest two stages in the mammalian brain evolution, being the  
4 first represented by the relatively big size of the cerebellum in non-mammaliaforms  
5 cynodonts (and the author suggest perhaps also the midbrain structures), reporting that  
6 even a cerebellum of the modern mammal *Didelphis virginiana* fits comfortably into the  
7 hind part of the endocranial cavity of the non-mammaliaform cynodont *Chiniquodon*.  
8 The cerebellar development could reflect the increase in the level of sophistication of  
9 the neuromuscular control of the movements associated to a more complex occlusion  
10 and the reorganization of the jaw musculature to create a bite that is simultaneously  
11 forceful and precise, as well as the locomotory system, including the more upright  
12 hindlimbs and the more mobile shoulder girdle with a wide range of possible forelimb  
13 movements. In this sense, the author mentioned the elaboration of the proprioceptive  
14 sensory input, and forward and backward feedback controls within the cerebellum  
15 (Mauk et al. 2000), suggesting new forward projections to the midbrain to be  
16 coordinated there with visual input, while the cerebral hemispheres remained  
17 primitively small, with no elaboration of cortical structures or development of a dorsal  
18 ventricular ridge. Regarding to the second stage, it is represented by the expansion of  
19 the telencephalic pallial structures to form the six-layered neocortex (isocortex) present  
20 in mammals (Kemp 2009).  
21  
22  
23  
24  
25  
26  
27  
28  
29  
30  
31  
32

33 Rowe et al. (2011), in turn, indicate three “pulses” in the evolution of the  
34 mammal brain, highlighting the non-mammalian mammaliaforms *Morganucodon* and  
35 *Hadrocodium*, as examples of two first pulses of encephalization determined by a  
36 significant widening in the region of the cerebral hemispheres and cerebellum, and a  
37 third pulse associated to the origin of the mammalian crown-group, with the presence of  
38 ossified ethmoturbinals, a cribriform plate and a rigid support in the nasal cavity to the  
39 olfactory epithelium receptor (OR). The activation of OR genes, which in mammals  
40 exceed by about one order of magnitude the amount existing in the genome of most  
41 other vertebrates (Niimura, 2009), induces the growth of the olfactory epithelium and  
42 turbinals, as well as their ossification (Rowe et al., 2005). According to these authors,  
43 the elaborate visual and auditory systems of mammals evolved later than these olfactory  
44 improvements. This is corroborated by Rodrigues et al. (2013), so that a stage, related to  
45 the neurological evolution related to olfactory accuracy, could be occurred later than the  
46 first stage indicated by Kemp (2009), and prior than the three pulses suggested by Rowe  
47 et al. (2011), represented by the increasing olfactory bulbs size, associated to more  
48 complex nasal cavity, and precursor to development of “superior” brain structures (i.e.  
49  
50  
51  
52  
53  
54  
55  
56  
57  
58  
59  
60

1  
2  
3 cerebral hemispheres) for sensorial processing and integration. Indeed, Jerison (1973)  
4 remarked that olfaction played a particularly significant role in the evolution of the  
5 mammalian brain, and associated this feature to the nocturnal habits of the small sized  
6 animals (i.e. non-mammalian mammaliamorphs).  
7  
8

9  
10 Moreover, Kemp (2009) also highlighted the process of miniaturization in  
11 Mesozoic cynodonts and its corresponding allometric consequences, including a non-  
12 reduction of the pressure over the occlusal surface area of the dentition (since the  
13 muscle force is related to cross sectional area, not to volume), and also neurological and  
14 sensorial effects, because a relatively larger space became available for cranial  
15 expansion between the epipterygoids as the adductor musculature of the temporal region  
16 became relatively smaller. These changes coincided with the need for a relatively larger  
17 endocranial cavity. Regarding the miniaturization, the author also suggested that the  
18 postdentary bones, reduced in mass, in addition to be free from a mechanical function as  
19 part of the lower jaw, rendered the system more sensitive to higher frequency sound.  
20  
21  
22  
23  
24  
25  
26  
27

### 28 **The role of *Riograndia guaibensis* in the evolution of the mammalian brain**

29  
30 *Riograndia* is the the most abundant cynodont taxon of the upper portion of the  
31 Candelária Sequence (early Late Triassic) of the Santa Maria Supersequence (Zerfass et  
32 al. 2003). Based on its abundance, it is used as reference taxon for the *Riograndia*  
33 Assemblage Zone (Soares et al. 2011) of Norian age (FIG 1).  
34  
35

36 Moreover, *Riograndia* is an important taxon to study of the transition between  
37 the non-mammaliaform cynodonts and the mammaliforms and the evolution of aspects  
38 of the mammalian biology within non-mammalian cynodonts by its phylogenetic  
39 relationships. In the phylogenetic analysis of Liu & Olsen (2010) *Riograndia* is the  
40 sister-taxon of a clade composed by *Pachygenelus* + ((*Brasilodon* + Mammaliaformes)  
41 + Tritylodontidae)). However, according to Martinelli & Rougier (2007), in an analysis  
42 including more ichthyosaurs, *Riograndia* was positioned as a non-Tritheledontidae, but  
43 within the group Ictidosauria. In effect, this taxon was originally described as an  
44 ictidosaur (Bonaparte et al. 2001) and it is one of the Mesozoic cynodonts that can be  
45 quoted with respect to the miniaturization and, consequently, its biological  
46 consequences. Furthermore, taking into account a sequence of the evolution of the  
47 mammalian brain observed within non-mammalian cynodonts, and the stages suggested  
48 based on the endocasts studied, as *Thrinaxodon*, *Probainoganthus*, *Brasilitherium* and  
49 different mammaliaforms, it was expected that *Riograndia* presents traits farther or  
50  
51  
52  
53  
54  
55  
56  
57  
58  
59  
60



1  
2  
3 closer to mammaliaforms, representing some intermediate stage in this evolutionary  
4 sequence.  
5  
6

## 7 8 **MATERIAL AND METHODS** 9

10  
11 The studied specimen (FIG. 3) belongs to the collections of the Laboratório de  
12 Paleontologia de Vertebrados of the Universidade Federal do Rio Grande do Sul  
13 (UFRGS) in Porto Alegre, Rio Grande do Sul state, Brazil. It was collected in the  
14 outcrop Sesmaria do Pinhal I (geographic coordinates: -29.684723°; -52.845851°;  
15 Datum WGS-84) near the town of Candelária, Rio Grande do Sul state, Brazil, and  
16 indicates the presence of the *Riograndia* Assemblage Zone (upper Candelária Sequence,  
17 Santa Maria Supersequence, Zeffass et al., 2003; Soares, et al. 2011; Horn et al. 2014).  
18 UFRGS-PV-0596-T consists of a virtually complete skull, with the right lower jaw  
19 ramus in occlusion, which is broken at the posterior half, just below the apex of the  
20 coronoid process, so lacking the angular process. Although the skull is well preserved,  
21 there is some parts broken and/or distorted due to post-mortem deformations: (1) the  
22 zygomatic arches are missing; (2) the quadrate ramus of the pterygoid, the epipterygoid  
23 (alisphenoid) and the cultriform process of the sphenoid complex (basisphenoid +  
24 parasphenoid) are absent; (3) in ventral view, the region of the interpterygoid vacuities  
25 can not be defined, as well the otic bones (prootic and opisthotic), lateral to the  
26 basisphenoid; (4) the ascendent process of alisphenoid and anterior process of prootic,  
27 can not be totally delimited on the lateral walls of the braincase, which are incomplete.  
28 Notwithstanding, these damages did not cause significant distortions in the overall  
29 endocast.  
30  
31  
32  
33  
34  
35  
36  
37  
38  
39  
40  
41  
42  
43  
44

### 45 **μCT scanning and digital extraction of the endocast**

46 The images were obtained from the CT Scanner NIKON XTH225ST located at  
47 the School of Earth Sciences, Life Sciences Building, University of Bristol, England.  
48 From the scanning were generated 1447 slices of the skull in coronal planes, with a  
49 resolution of 1,024 x 1,024 pixels and a pixel size of pixel size 0.0239904 x 0.0239922  
50 mm.  
51  
52  
53

54 The visualization of the slices, 3D rendering, measurements, segmentation and  
55 treatment of the images to separate the rocky matrix from the bony elements were  
56 performed using the softwares VGStudio Max (version 1.2.1; Volume Graphics GmbH)  
57  
58  
59  
60

1  
2  
3 and Avizo (Standart Edition, version 7.1.0, FEI Visualization Sciences Group). The  
4 brain endocast was reconstructed using the infilling material in the cranial cavity. The  
5 slices were also manually treated in order to remove, from the segment corresponding to  
6 the endocast, external elements with similar density (gray scale) of the internal rocky  
7 matrix.  
8  
9

10  
11 Two volumes of the endocast were calculated, one taking into account the whole  
12 cast behind the posterior limit of the nasal cavity, and other without the filling of the  
13 orbital vacuity above the pterygoids, which was digitally removed. In this way, the  
14 ventral contour of the olfactory bulb casts was setted based on this dorsal morphology,  
15 assuming that the bulbs were dorsoventrally symmetrical in lateral view. The same  
16 criterium was used by Rodrigues et al. (2013) for *Brasilitherium*, taking into account  
17 that in endocasts described in the literature the olfactory bulbs usually have a ventral  
18 contour similar to the dorsal contour in lateral view (e.g., Quiroga 1979, 1980a, b, c,  
19 1984; Macrini et al. 2006, 2007a, b; Rowe et al. 2011), as well as the actual ventral  
20 extension of the olfactory bulbs region delimited, in non-mammaliaforms, cynodonts  
21 with ossified orbitosphenoid forming a floor for this region as travesodontids (e.g. Luo  
22 1994) and *Chiniquodon* (e.g. Kemp, 2009). In *Riograndia* UFRGS-PV-596-T, the  
23 estimated ventral extension of the olfactory bulbs region does not differ significantly  
24 from the ventral limit of the cast left by the orbital process of the frontal bones.  
25  
26  
27  
28  
29  
30  
31  
32  
33  
34  
35  
36  
37

### 38 **Quantitative analysis**

39 To calculate the EQ for *Riograndia*, it was necessary to estimate its body mass  
40 first. Because we do not have postcranial bones associated with any of the known skulls  
41 for this taxon, the body mass was estimated from the skull length using the equation  
42 utilized by Luo et al. (2001) for the Jurassic mammaliaforms *Sinoconodon*,  
43 *Morganucodon* and *Hadrocodium* and Rodrigues et al. (2013) for *Brasilitherium*:  $X =$   
44  $3.68Y - 3.83$ , where X is the log<sub>10</sub> of the body mass in grams and Y is the logarithm of  
45 the skull length in millimeters (this is a regression equation based on the scaling  
46 relationship of body mass to skull size in 64 species of living lipotyphlan insectivore  
47 mammals presented by Gingerich and Smith, 1984).  
48  
49  
50  
51  
52  
53

54 The EQ was calculated from the endocast volume (EV) and the estimated body  
55 mass (BM), which was obtained using two different equations:  $EQ = EV/0.12BM^{0.67}$ ,  
56 from Jerison (1973), and  $EQ = EV/0.055BM^{0.74}$ , from Eisenberg (1981), as presented  
57  
58  
59  
60

1  
2  
3 in Table 2. However, comparisons with EQs of non-mammalian cynodonts are  
4 difficult, as showed by Rodrigues et al. (2013), since the endocast of *Brasilitherium* is  
5 clearly larger related to the skull, and its EQ agrees with an evolutionary sequence from  
6 non-mammalian cynodonts to increasing EQs in the taxa more closely related to  
7 mammals, so that the EQs of *Diademodon* and *Massetognathus* calculated by Jerison  
8 (1973) and Quiroga (1979, 1980c), respectively, seems to be overestimated, probably  
9 due to the equation to estimate the body mass.  
10

11  
12  
13  
14 Thus, due to the imprecisions of the endocast volumes and, mainly, to estimate  
15 the body mass of different taxa from different equations, we try another way of  
16 comparing the relative size of the olfactory bulb cast on the brain endocasts, in order to  
17 compare the relative size of brain structures, mainly the olfactory bulbs, considering the  
18 importance of the olfactory bulbs and the increment of the olfaction sense in the  
19 transition between non-mammalian cynodonts and the Mammaliaformes lineage.  
20 For this purpose, given the similar endocast general design of non-mammalian  
21 cynodonts, it was measured the length and area of the dorsal exposition of the olfactory  
22 bulbs, cerebral hemisphere and cerebellar regions, as well as of whole brain endocast in  
23 dorsal view. This measurements was realized in *Riograndia* UFRGS-PV-596-T and  
24 other non-mammalian cynodont taxa, from digitalized pictures showing the dorsal view  
25 of the endocast in other works (*Hadrocodium*, Macrini, 2006; *Brasilitherium*, Rodrigues  
26 et al. 2013; *Therioherpeton*, Quiroga, 1984; *Probainognathus*, Quiroga, 1980a, b;  
27 *Probelesodon* and *Massetognathus*, Quiroga, 1979, 1980c) - using the software  
28 Digimizer (Version 4.6.1, MedCalc Software BVBA). In order to standardize the  
29 comparison parameters, we obtained ratios of the measurements taken in relation to the  
30 skull length, as well as the measurements of the regions of the endocast between them  
31 and related to the whole endocast for each taxon. These ratios are showed in the Table 3.  
32  
33  
34  
35  
36  
37  
38  
39  
40  
41  
42  
43  
44

## 45 46 DESCRIPTION AND COMPARISONS

### 47 48 General aspects

49  
50 The endocranial cast of *Riograndia* UFRGS-PV-596T, in dorsal view (FIG. 4A),  
51 can be delimited between the foramen magnum and a groove, observed in dorsal and  
52 lateral view, which marks the anterior limit of the olfactory bulb casts. This groove  
53 results from an internal thickening of the frontal bone, which forms a ventrally directed  
54  
55  
56  
57  
58  
59  
60

1  
2  
3 ridge visible in lateral section, while their dorsal surface on the roof of the skull  
4 remains flat, transversely aligned between the orbital processes on both sides. Thus,  
5 the nasal cavity and the brain cavity are partially separated at the roof of the skull,  
6 despite the lack of an ossified cribiform plate (which appears only in mammals; e.g.  
7 Rowe, 1988; Kielan-Jaworowska et al. 2004). However, there is not a crest in the  
8 internal surface of the skull roof which could indicate the presence of a median sulcus  
9 separating the cerebral hemispheres and the olfactory bulb casts.  
10  
11  
12  
13

14  
15 The general shape of the dorsal surface of the endocast is anteroposteriorly  
16 elongated, being the aspect ratio between the maximum width and length approximately  
17 0.4. The endocast is gradually wider posteriorly until the anterior limit of the cerebellar  
18 region, which presents a rounded lateral contour so that the width from this point  
19 decreases to the foramen magnum. The length of the endocranial cast, between the  
20 anterior limit of the dorsal surface of the olfactory bulbs and the foramen magnum is  
21 16.31 mm, corresponding to 44% of the total length of the skull (35.08 mm). The  
22 maximum width is 6.88 mm, at the anterior limit of the cerebellar region, where there is  
23 a conspicuous transversal linear structure, here interpreted as a vascular cast (see the  
24 specific title, below). Behind this mark of the endocast is the cerebellar region to the  
25 foramen magnum, where is the maximum width excluding the vascular mark (6.20  
26 mm), there are two lateral structures, corresponding to the parafloccular casts, which fill  
27 the fossa subarcuata. Contrary to *Brasilitherium* (Rodrigues, 2013), these structures are  
28 not conspicuous in *Riograndia* PV-596T.  
29  
30  
31  
32  
33  
34  
35  
36  
37  
38

39 The lateral profile of the endocranial cast of the specimen *Riograndia* UFRGS-  
40 PV-596T reveals a slightly anteroposterior convex dorsal surface at the olfactory bulbs  
41 region, so that is possible estimate their posterior limit (although the measurement of  
42 the length of the olfactory bulbs can be obtained with more precision from the 2D slices  
43 images). Behind this region, the dorsal contour becomes straight, with a slight slope in  
44 the posterior direction ( $5.48^\circ$  relative to a hypothetical dorsal horizontal plane from the  
45 posterior limit of the olfactory bulb casts) along 6.95 mm and so the slope becomes  
46 much steeper ( $24.10^\circ$ , from their top, and  $9.12^\circ$  relative to a hypothetical dorsal  
47 horizontal plane from the posterior limit of the olfactory bulb casts) for about 1.91 mm.  
48 The lowest point of this slope is interpreted as the mark of the posterior limit of the  
49 brain hemispheres region. Immediately behind that slope, there is a ridge, on a level  
50 most dorsal than the adjacent surfaces (anterior and posteriorly), on a level equivalent to  
51  
52  
53  
54  
55  
56  
57  
58  
59  
60

1  
2  
3 the region of the cerebral hemispheres anterior to the slope, which corresponds to the  
4 vascular mark (discussed below). This mark in lateral view is a ridge, from which, in an  
5 antero-posterior direction, the dorsal contour of the endocast makes a slope backwards  
6 (59.24°), along 4.68 mm, to the level of the foramen magnum  
7  
8

9  
10 The ventral limit of the anterior half of the endocast cannot be determined, due  
11 to the presence of a space not ossified between the pterygoid and the frontal (i.e. the  
12 orbital vacuity). Posteriorly to this space, in a lateral view of the skull, there is the  
13 ascendant process of the alisphenoid, and ventrally, the endocast is delimited by the  
14 basicranial bones (basisphenoid/parasphenoid, basioccipital, prootic and opisthotic).  
15 Between the orbital vacuity and the paraflocculus cast, no neuroanatomical details are  
16 distinguishable in lateral view.  
17  
18

19  
20  
21 In ventral view, there is no relevant detail discernible on the surface, since the  
22 basicranial bones are distorted and broken. The hypophyseal fossa (filling of the sella  
23 turcica) can be observed in some 2D images (slices), and so, can be located on the 3D  
24 endocast reconstruction, but the hypophyseal cast not appears as a prominent structure  
25 as *Brasilitherium* (Rodrigues et al., 2013), but this may due to the damaged  
26 basicranium of this specimen, mainly on the basisphenoid bone. In addition, there is not  
27 a clear cast of the ventral opening of the cavum epitericum in both sides, because the  
28 quadrate rami of pterygoids and alisphenoid were broken. Thus, most of the space  
29 filling of the semilunar ganglion of the trigeminal nerve, lateral to the wall formed by an  
30 anterior extension of the prootic (i.e. the pila antotica) that delimits the intracranial  
31 space proper (Presley 1980; Maier 1987; Novacek 1993; Rougier and Wible, 2006), was  
32 not considered as compounding the volume of this endocast. The length of the ventral  
33 opening of the cavum epitericum could be measured (= 5 mm), not on the endocast,  
34 but considering the opisthotic as the posterior limit, and the most anterior portion of the  
35 quadrate ramus of pterygoid as the anterior one. The most posterior region of the  
36 endocast, delimited by the basioccipital, has a rounded surface, with a more pronounced  
37 bulge along a central longitudinal band. This region represents the ventral surface of the  
38 hindbrain and surrounding tissues (mainly meninges), but is not possible to identify  
39 specifically the medulla oblongata and the pons.  
40  
41  
42  
43  
44  
45  
46  
47  
48  
49  
50  
51  
52  
53  
54  
55

### 56 **Forebrain region**

57  
58  
59  
60

1  
2  
3 The portions of forebrain which left visible impressions on the endocast  
4 described are the olfactory bulbs and the cerebral hemispheres. The most anterior part of  
5 the endocranial cast represent the space occupied by the olfactory bulbs and associated  
6 meninges (Macrini et al., 2007b). Despite the absence of an ossified cribriform plate in  
7 the skull, separating the nasal cavity from the braincase, the definition of the anterior  
8 limit of the olfactory bulbs could be observed in dorsal and lateral view, as mentioned  
9 above. In spite of the external surface of the skull roof, the dorsal contour of the  
10 posterior end of the nasal cavity is clearly at a level taller than the anterior limit of the  
11 olfactory bulb in lateral view, separated by a deep fossa in the dorsal surface of the  
12 endocast. Moreover, there is two rounded casts on the dorsal surface, corresponding to  
13 the two bulb casts, although the longitudinal groove between them is not so clear in  
14 dorsal view. Regarding this aspect, *Brasilitherium* (Rodrigues et al. 2013) presents a  
15 sulcus clearly deeper than *Riograndia*, but this taxon do not differs significantly from  
16 other non-mammalian eucynodonts as *Probelesodon* and *Massetognathus*, for  
17 which Kielan-Jaworowska *et al.* (2004) indicate olfactory bulb casts more developed  
18 and better separated from each other when compared to *Thrinaxodon*.

19  
20  
21 The region of the olfactory bulbs can be delimited, both in lateral view, due to a  
22 gentle dorsal convexity in the contour, and in the dorsal view, due to a slight transversal  
23 constriction, which seems the circular fissure (sensu Loo 1930; Rowe 1996; also called  
24 transverse furrow, sensu Kielan-Jaworowska, 1986; transverse sulcus, sensu Krause and  
25 Kielan-Jaworowska 1993; or circular sulcus, sensu Luo et al. 2002). A well-defined  
26 circular fissure, although usually present in mammals (Macrini et al., 2007b), but is not  
27 described for other non-mammalian cynodonts (Quiroga, 1979, 1980a, b, c), and  
28 even is ambiguous in *Brasilitherium*, in which this area has a width similar to the region  
29 immediately posterior to it (Rodrigues et al. 2013). In *Riograndia* UFRGS-PV-596-T, in  
30 turn, the width of the dorsal surface at this point is 3.85 mm, while the maximum width  
31 of the olfactory bulbs region is 4.12 mm, and the endocast becomes also wider in  
32 backward direction from this point. The olfactory bulb casts of *Riograndia* UFRGS-PV-  
33 596-T, in dorsal view, are two oval structures anteroposteriorly elongated (FIG. 4A),  
34 being the ratio of the maximum width and length equal to 0.38 and 0.34, for the bulb  
35 casts left and right, respectively. The maximum width of the two olfactory bulb casts  
36 together is 4.12 mm, measured at half the length of the bulb casts, while the width near  
37 to the anterior limit of the olfactory bulb casts is 3.64 mm.

1  
2  
3 Due to the lack of an ossified floor in the most anterior region of the skull, there  
4 is also no impression of the olfactory tracts (Butler and Hodos, 1996), from the  
5 olfactory bulbs to the telencephalon region. In fact, the olfactory tracts do not usually  
6 leave impressions in endocasts of mammals because they are hidden by the meninges  
7 (Macrini et al., 2007b), but the posterior limit of the olfactory bulb casts immediately  
8 anterior to the cerebral hemispheres region, as viewed in *Riograndia* UFRGS-PV-596-  
9 T, allow us to infer the presence of the olfactory tracts ventral to the bulbs. With respect  
10 to this feature, we can consider as plesiomorphic within cynodonts the patten described  
11 for *Massetognathus* (Quiroga, 1979, 1980c) and *Exaeretodon* (Bonaparte, 1966), with  
12 the olfactory tracts forming a peduncle between the olfactory bulb casts and the region  
13 of the cerebral hemispheres, as occurs in many living reptiles (Hopson, 1979; Kielan-  
14 Jaworowska et al., 2004). The ventral boundary of the olfactory bulb casts can not be  
15 accurately identified due to the lack of an ossified floor for the olfactory bulbs, despite  
16 the presence of an ossified orbitosphenoid indicated by Soares et al. (2011), because  
17 this bone in *Riograndia*, in addition to having a more ventral position compared to other  
18 non-mmmalian cynodonts (e.g. Hopson, 1964; Sues, 1986; Kielan-Jaworowska et al.,  
19 2004; Oliveira et al., 2010), below the orbital process of the frontal , consists of a lateral  
20 lamina with no medial projection.  
21  
22  
23  
24  
25  
26  
27  
28  
29  
30  
31  
32

33 The region of the cerebral hemispheres in dorsal view extends 7.53 mm to the  
34 transversal vessel impression, intified as the posterior limit. The dorsal surface is flat,  
35 with a very little pronounced median sulcus (=longitudinal fissure) dividing the region  
36 into two casts of distinct hemispheres. The division in two casts becomes more evident  
37 closer to the posterior limit, at a point 6.95 mm from the limit between the cerebral  
38 hemispheres region and the olfactory bulb casts, from which two bulging surfaces  
39 diverge laterally, about 20° from the medial line, along 1.9 mm, leaving a very small  
40 lower central space, which forms a half-circle, whose transverse line is delimited by the  
41 elevation of the vascular cast which passes through the dorsal surface of the endocast  
42 transversally. The point of maximum divergence is the maximum width of the cerebral  
43 hemispheres region with 5.25 mm, while the width of the endocast at the limit between  
44 the cerebral hemispheres region and the olfactory bulb casts is 3.9 mm. The lateral  
45 profile shows that cerebral hemispheres region is lower than the convex surface of the  
46 olfactory bulb casts and the dorsal surface is approximately straight along 5.82 mm, to a  
47 point from which an accentuated slope (24.10° from the anterior straight portion),  
48  
49  
50  
51  
52  
53  
54  
55  
56  
57  
58  
59  
60

1  
2  
3 corresponding to the portion of divergence of the hemisphere casts visible in dorsal  
4 view. The non-mammaform cynodonts *Thrinaxodon* (Kielan-Jaworowska et al., 2004),  
5 *Massetognathus* (Quiroga, 1979, 1980c), *Exaeretodon* (Bonaparte, 1966), and  
6 *Probelesodon* (Quiroga, 1979, 1980c) do not present a division in this region of the  
7 endocast, but the presence of two distinct hemispheres is described for *Probainognathus*  
8 (Quiroga, 1980a, b) and *Brasilitherium* (Rodrigues et al., 2013). In this last taxon the  
9 median sulcus is very pronounced (although considered not so deep as to indicate the  
10 presence of an ossified falx cerebri as different lineages of living mammals (e.g.  
11 Macrini et al., 2007b). On the other hand, the ratio between the maximum width and the  
12 length of the dorsal surface of the cerebral hemispheres region is higher in *Riograndia*  
13 than other non-mammaliaform cynodonts, *Massetognathus*, *Probelesodon*,  
14 *Probainognathus*, *Therioherpeton* and *Braislitherium* (see Table 3).  
15  
16  
17  
18  
19  
20  
21  
22

23 Since the dorsal surface of the cerebral hemispheres region is flat, there is not  
24 any mark indicating a pineal body, which is associated parietal eye and includes the  
25 portion of the epithalamus (Butler and Hodos, 1996) of the diencephalon, having  
26 thermoreceptive functions that regulate circadian rhythms and reproductive cycles (Roth  
27 et al., 1986; Butler and Hodos, 1996). In fact, the clear evidence of the pineal body in  
28 endocasts is the parietal foramen, opening to the parietal eye (Roth et al., 1986), which  
29 is absent in most eucynodonts (exceptions, *Cynognathus*, *Pascualgnathus*, and  
30 *Diademodon*, e.g., Bonaparte et al., 2005; Abdala, 2007), although a cast of a parietal  
31 tube is indicated in the parietal endocranial cast of *Massetognathus* (Quiroga, 1979,  
32 1980c) and a pineal region, behind the median sulcus, at the most posterior region of the  
33 cerebral hemispheres, was suggested by Quiroga (1980b, c) for *Probainognathus*.  
34  
35  
36  
37  
38  
39  
40  
41

42 Furthermore, as would be expected, there is no mark of the rhinal fissure, which  
43 corresponds to the ventral boundary of the isocortex (neocortex), nor markings  
44 indicating the presence of cerebral gyri and sulci, the convolutions of the cortex and the  
45 grooves between the gyri, respectively (Butler and Hodos, 1996). Despite the possibility  
46 of endocasts do not reflect the convolutions of the real brains (e.g., *Tursiops truncatus*,  
47 Colbert et al., 2005), it is expected that non-mammalian cynodonts have had  
48 lissencephalic surfaces (smooth cortical brain surfaces) because this condition is  
49 considered plesiomorphic for the mammalian crown-group (Kielan-Jaworowska et al.,  
50 2004). Regarding to the rhinal fissure, the presence of a neocortex (isocortex) in a non-  
51 mammaliaform cynodont was suggested only for *Probainognathus* by Quiroga (1980b),  
52  
53  
54  
55  
56  
57  
58  
59  
60



1  
2  
3 based on the presence of a groove which would mark the posterior limit of that region,  
4 but it has been contested and the groove has been considered as a mark of a blood vessel  
5 in the external surface of the brain (Kielan-Jaworowska, 1986). A rhinal fissure can also  
6 be present in brains without appearing in the respective endocasts (Jerison, 1991), but is  
7 also expected that it is present only among taxa of the mammalian crown-group  
8 (Macrini et al., 2007b). Moreover, in ventral view, no feature of the forebrain can be  
9 observed.  
10  
11  
12  
13

### 14 15 16 17 **Midbrain Region**

18  
19 The portion of the midbrain exposed on the dorsal surface of the endocasts  
20 corresponds mainly to the anterior and posterior colliculi. Although these structures  
21 may be exposed on the dorsal surface of the brain but does not appear in endocasts,  
22 even in living taxa (e.g. *Didelphis virginiana*, Dom et al., 1970; *Monodelphis*  
23 *domestica*, Macrini et al., 2007a; *Tenrec ecaudatus*, Bauchot and Stephan, 1967), the  
24 presence of casts of these structures is described for several extinct mammals e.g.,  
25 *Labidolemur* (Silcox et al., 2011), *Kennalestes* (Kielan-Jaworowska, 1984, 1986),  
26 *Asioryctes* (Kielan-Jaworowska, 1984), and *Zalambdalestes* (Kielan-Jaworowska, 1984,  
27 1986). However, the midbrain may not be visible in endocasts because it is covered by  
28 meninges, blood sinuses or due to the presence of a telencephalon posteriorly expanded  
29 or an anteriorly expanded cerebellum (Edinger, 1964).  
30  
31  
32  
33  
34  
35  
36  
37

38 Regarding to non-mammalian cynodonts, the only suggestion of midbrain  
39 exposition in a non-mammalian cynodont is for *Probainognathus* by (Quiroga 1980b,  
40 c), but according to Macrini et al. (2007b), the plesiomorphic condition for the  
41 mammalian crown-group should be the no exposure of the midbrain. For  
42 *Brasilitherium*, Rodrigues et al. (2013) found no evidence of exposure of the midbrain,  
43 considering it more likely to be covered by telencephalon, since the casts of the cerebral  
44 hemispheres appear to extend to the cerebellar region in dorsal view. Moreover, the  
45 median sulcus appears continuous along the the cerebral hemispheres region of  
46 *Brasilitherium*, without a central wider depression, which is observed in  
47 *Probainognathus* (Quiroga 1980b), between the hemispheres casts at their most  
48 posterior portion.  
49  
50  
51  
52  
53  
54  
55  
56  
57  
58  
59  
60

1  
2  
3 In *Riograndia* UFRGS-PV-596-T, there is no direct evidence of midbrain  
4 exposition, as well as a pineal region as suggested by Quiroga (1980b, c) for  
5 *Probainognathus*. The small lower space amid the lateral divergence between the  
6 hemispheres casts at their posterior end could have a little extension posteriorly, perhaps  
7 becoming wider and representing the midbrain dorsal exposition, however, according to  
8 our interpretation, the transversal vascular cast (transversal ridge on the endocast) covers  
9 the surface between the posterior boundary of the cerebral hemispheres and the most  
10 anterior dorsal surface of the cerebellar region.  
11  
12  
13  
14  
15  
16  
17  
18

### 19 **Hindbrain Region**

20  
21 The hindbrain region appears, in dorsal view, posteriorly to the slope of the  
22 cerebral hemispheres casts, just behind the transverse ridge (vascular cast, see below).  
23 The parafloccular cast, which fills the fossa subarcuata at the ascendant process of  
24 prootic, is posterior to the lateral continuity of the ridge, as structures that detach (0.72  
25 mm at left side, and 0.74 mm at right side) from the lateral surface of this region of the  
26 endocast, constituting its widest point. From the parafloccular cast to the foramen  
27 magnum lateral contour is rounded. The dorsal surface is convex laterally, with no  
28 detail conspicuous (as could be, for example, a division of cerebellar hemispheres,  
29 which was indicated in *Probainognathus* (Quiroga, 1980a, b), although it is not clear in  
30 others non-mammaliaform cynodonts).  
31  
32  
33  
34  
35  
36  
37

38 In any case, the dorsal surface has a slight bulging in the more central portion  
39 (approximately 1/3 of the endocast width on this region), which could correspond to the  
40 vermis of the cerebellum, as suggested for *Brasilitherium* (Rodrigues et al, 2013). The  
41 vermis, as well as the lateral cerebellar hemispheres are not characterized as specialized  
42 structures, functionally distinct from the rest of the cerebellum (Butler and Hodos,  
43 1996). However, they are structures that can be marked in endocasts, and their presence  
44 within non-mammalian cynodonts can be associated with the degree of development of  
45 the cerebellum in different taxa along the evolution of the mammalian lineage. Thus,  
46 although a vermis has not been identified in many descriptions of endocasts of non-  
47 mammalian cynodonts (Watson 1913; Hopson 1979, Quiroga 1979, 1980a, b, c, 1984),  
48 Kielan-Jaworowska et al. (2004) indicate its presence in the endocast of *Thrinaxodon*,  
49 represented by a protuberance in the posterior part of the dorsal surface, which fills a  
50 non-ossified area covered by the parietal and partly by the interparietal. However, Rowe  
51  
52  
53  
54  
55  
56  
57  
58  
59  
60

1  
2  
3 et al. (1995) suggested that the dorsal space between the parietal and interparietal bones  
4 marks the position of a superior sagittal sinus. As mentioned below, we interpreted the  
5 filling of this unossified zone as a vascular cast, so that the vermis could be dorsally  
6 exposed behind this mark, represented by the central bulging, probably partially covered  
7 by the blood vessels.  
8  
9

10  
11 Regarding to the parafloccular casts, they are not so conspicuous as in  
12 *Brasilitherium* (Rodrigues et al. 2013). Although the degree of filling of the fossa  
13 subarcuata can be variable in different mammals (e.g. Sanchez-Villagra 2002), this  
14 feature, in endocasts, is associated with the degree of development of the paraflocculi  
15 lobes (Kielan-Jaworowska et al. 2004), which is associated with coordination, balance  
16 and vestibular sensory acquisition (Butler and Hodos, 1996). The parafloccular casts are  
17 absent in the endocasts of some non-therapsid cynodonts, often due to the poor  
18 ossification of this region of the skull (Kielan-Jaworowska et al., 2004), but the  
19 presence of prominent paraflocculi is a plesiomorphic condition for eucynodonts, as is  
20 described for *Thrinaxodon* (Rowe, 1996) and *Nyctosaurus* (Hopson 1979), and all other  
21 non-eucynodont mammaliaformes with endocasts described (e.g., Quiroga, 1979, 1980a,  
22 b, c, - identified as “flocculi” in these works). Although less prominent than  
23 *Brasilitherium*, the lateral projection of the endocast of *Riograndia* UFRGS-PV-596-T  
24 seems to be similar to the parafloccular casts of *Probelesodon* and *Probainognathus*,  
25 but Quiroga (1980a, b) reconstitute these structures as a more elongated projection,  
26 directed more posteriorly, as visible in the endocast itself of *Massetognathus* (Quiroga,  
27 1979, 1980c), while in *Riograndia* they appear as a lateral prominence. In  
28 *Brasilitherium*, the parafloccular casts are perfectly defined and not so posteriorly  
29 directed (posterolaterally oriented away from the longitudinal axis of the endocranial  
30 cast by approximately 40°-60°, Rodrigues et al, 2013)  
31  
32  
33  
34  
35  
36  
37  
38  
39  
40  
41  
42  
43  
44  
45  
46  
47

#### 48 **Vascular marks on the endocast**

49 As already mentioned, the endocast of *Riograndia* presents a ridge, which passes  
50 through the endocast transversely, in dorsal view, just behind the cerebral hemispheres  
51 casts, and, in lateral view, is on a level most dorsal than the adjacent surfaces, i.e. the  
52 slope (24.10°) of the posterior end of the cerebral hemisphere casts, anteriorly, and the  
53 slope of the dorsal surface of the cerebellar region (59.24°) to the foramen magnum.  
54 The 2D slices of this portion of the skull in lateral and coronal planes shows (FIG. 5)  
55  
56  
57  
58  
59  
60

1  
2  
3 that is the region of the unossified zone, delimited anteriorly and dorsally by the  
4 parietal, and posteriorly by the parietal and supraoccipital, , having, most of the space, a  
5 position more dorsal than the last. This space is a common feature of the non-  
6 mammaliaform cynodonts, a dorsal region of the supraoccipital roofed by the parietal  
7 and perhaps partly the interparietal. (e.g. Kemp, 2009) and, as mentioned above, it can  
8 left a mark on the endocast of non-mammalian cynodonts interpreted as a cerebellar  
9 vermis cast (e.g. Kielan-Jaworowska et al., 2004) or the sagittal sinus (Rowe et al.  
10 1995).

11  
12  
13 In *Riograndia* UFRGS-PV-596-T, a transversal ridge is visible in dorsal view,  
14 whose posterior slope extends by 1.66 mm, but only in the medial portion,  
15 corresponding to about 1/3 of the width of the endocast in this region. and covering part  
16 of the posterior adjacent dorsal surface of the endocast, which forms a slope of 4.68 mm  
17 to the foramen magnum. In addition, this central structure has lateral continuity, 1/3 of  
18 the ridge each side in dorsal view, as a narrower transversal ridge, which extends to the  
19 lateral walls of the endocast. These transversal continuities of the ridge are slightly  
20 curved lateroposteriorly and extend ventrally approaching the parafloccular casts.  
21  
22  
23  
24  
25  
26  
27  
28  
29

30  
31 We suggest that the transversal ridge as a vascular cast, corresponding to the  
32 transverse sinus. In addition, taking into account this transversal vascular cast, the most  
33 central portion, which extends backwards, and fills the unossified zone, it is  
34 interpreted here as the transverse sinus, which is a dorsal continuation of the prootic  
35 sinus (e.g. Wible & Hopson 1995), but there is no mark of the cast of this vessel on the  
36 lateral wall of the endocast of *Riograndia* UFRGS-PV-596-T. The prootic sinus cast  
37 was identified in the endocast of *Brasilitherium* (Rodrigues et al. 2013).  
38  
39  
40  
41  
42  
43  
44  
45

#### 46 **Relative size of the brain cast and their structures**

47  
48 The volume of the whole endocast is 445.45 mm<sup>3</sup> and the volume of the  
49 endocast with the filling of the orbital vacuity above the pterygoids digitally removed is  
50 404.20 mm<sup>3</sup> (FIG 4D). Thus, from a body mass estimated in 71.15 g, we obtained four  
51 values of EQs, two using the equation of Jerison (1973), 0.22 and 0.20, and two through  
52 the equation of Eisenberg (1981), 0.30 and 0.33 (Table 2).  
53  
54  
55

56  
57 Comparatively, the EQs calculated for *Riograndia* are higher (0.20 without the  
58 filling of the orbital vacuity, and 0.22, endocast complete) than the EQ calculated  
59  
60

1  
2  
3 through the same equation for the non-mammalian cynodonts for *Thrinaxodon*  
4 (0.10; Jerison, 1973), *Diademodon* (0.14, Quiroga, 1980b), *Massetognathus* (0.15;  
5 Quiroga, 1979, 1980c); *Exaeretodon* (0.10 and 0.15; Quiroga, 1980b), *Probelesodon*  
6 (0.13 and 0.18; Quiroga, 1979, 1980c), *Probainognathus* (0.12 and 0.17; Quiroga  
7 1980a, b). However, the values of *Diademodon* (0.21) calculated by Jerison (1973), and  
8 one of the values, based on another body mass estimate, calculated by Quiroga (1979,  
9 1980c) for *Massetognathus* (0.22), are higher than the EQs of *Riograndia*. Among  
10 mammalian forms, the EQs of *Riograndia* are higher than *Brasilitherium* (0.15 and 0.22,  
11 for the equations of Jerison, 1973, and Eisenberg, 1981, respectively) and the value of  
12 the endocast complete (0.33) exceeds *Morganucodon* (0.32, Rowe et al. 2011), using the  
13 same equation to calculate the EQ. Furthermore, *Riograndia* presents a lower EQ  
14 compared to other mammalian forms (Table 2).  
15  
16  
17  
18  
19  
20  
21  
22

23  
24 Moreover, regarding to the relative size of the olfactory bulbs, Macrini et al.  
25 (2007b) used the ratio, in relation to the total volume of the endocranial cast, as a  
26 character in their phylogenetic analysis, defining the states discreetly, with reference to  
27 an average of 6%, and the primitive state corresponding to a size greater than or equal to  
28 6%. However, the authors state that the plesiomorphic condition corresponds to the  
29 primitive mammalian morphology, and the derivate state were acquired convergently in  
30 those lineages and are presumably related to the reduced sense of smell in aquatic  
31 mammals (Negus, 1958; Pirlot and Nelson, 1978; Meisami and Bhatnagar, 1998;  
32 Macrini et al. 2007b). On the other hand, as highlighted by Rodrigues et al. (2013),  
33 among non-mammalian cynodonts there is a great variation, with the volume of the  
34 olfactory bulb casts corresponding to 5% of the endocranial cast in *Massetognathus*,  
35 19.7% in *Exaeretodon*, 7.8% in *Probelesodon*, 6.4% in *Probainognathus* (Quiroga,  
36 1980b), and 35.8% in *Brasilitherium* (Rodrigues et al., 2013), while the percent of  
37 endocast composed by olfactory bulb casts is 14.22 in the non-mammalian  
38 mammalian form *Hadrocodium* (Macrini 2006). In *Riograndia*, the volume of the  
39 olfactory bulbs region (with the ventral contour digitally delimited) is 79.49 mm<sup>3</sup>,  
40 corresponding to 19.67% of the volume of the endocast without the the rocky filling of  
41 the orbital vacuity.  
42  
43  
44  
45  
46  
47  
48  
49  
50  
51  
52

53  
54 Besides, the area of the dorsal exposure of the olfactory bulbs region is 19.4% of  
55 the dorsal surface of the whole endocast, being the regions of the cerebral hemispheres  
56 and cerebellum, 66.7% and 13.9% of the dorsal surface of the endocast, respectively.  
57  
58  
59  
60

1  
2  
3 The comparison with other cynodont taxa, regarding to the area of dorsal exposure of  
4 the endocast and their regions related to the skull length is showed in the Table 3.  
5

6  
7 The results of the approach proposed here (evolving three non-prozostodontia  
8 cynodonts, three prozostodontian non-mammaliaforms, one basal mammaliform, and  
9 one crown mammalian) are summarized on the Table 3, are remarked separately, for the  
10 endocasts and the different regions of the brain identified in dorsal view.  
11  
12

### 13 14 15 16 The whole endocast

17  
18 Related to the skull length, the endocast length is, in general, relatively larger the  
19 smaller the skull, corresponding to a larger nasal cavity (related to the length of the  
20 endocranial space) the larger the size of the skull. This ratio is better adjusted in a linear  
21 regression with the exception of *Therioherpeton*, which has the relatively longer  
22 endocast among the taxa sampled, as well as *Riograndia* and *Brasilitherium*, in which  
23 the relatively more elongated nasal cavity. Moreover, regarding to the aspect ratio  
24 taking the maximum width and length, the relationship is also proportional to the size of  
25 the skull, so that smaller skulls have relatively wider endocranial space. However, in  
26 this case, a phylogenetic influence may be suggested, since a regression line with a high  
27 coefficient of determination ( $R^2 = 0.98$ ) can be obtained for non-mammaliaform  
28 cynodonts, while *Hadrocodium* (the smallest sample skull) and *Vincelestes* (with a skull  
29 of intermediate size between the specimens compared, similar to *Probainoganthus*)  
30 present relatively wider endocasts (see graphic in the Appendix 1).  
31  
32  
33  
34  
35  
36  
37  
38  
39  
40  
41  
42

### 43 The olfactory bulbs region

44  
45 The length of the olfactory bulbs region related to the skull length is also  
46 relatively larger the smaller the skull ( $R^2=0.93$ ) Thus, the bulbs are relatively longer in  
47 relation to the skull the longer the relative length of the endocranial space, but,  
48 regarding to this relationship, *Brasilitherium* stands out above the regression line,  
49 which can corroborate the suggestion of Rodrigues *et al.* (2013) that this taxon presents  
50 the largest relative size of olfactory bulbs within cynodonts, including mammaliaformes,  
51 with endocasts described.  
52  
53  
54  
55  
56  
57  
58  
59  
60

1  
2  
3 In addition, *Brasilitherium* presents the highest value for the ratio of the area of  
4 the olfactory bulbs region on dorsal view and the area of the dorsal surface of the whole  
5 endocast (0.35). In effect, this ratio appear to be, in general, higher for non-  
6 mammaliaform cynodonts successively more related to mammals, although the value of  
7 *Probelesodon* (0.29) is higher than *Probainognathus* (0.22) and of *Therioherpeton*  
8 (0.34) is higher than *Riograndia* (0.30). Among mamaliaformes, this same ratio  
9 becomes much lower in *Hadrocodium* and even lower in *Vincelestes*.

#### 14 The cerebral hemispheres region

15  
16  
17  
18  
19 The ratio of the area of the cerebral hemispheres region on dorsal view and the  
20 area of the dorsal surface of the whole endocast, seem to present a clear change among  
21 mammaliaformes, in which the relative area of the cerebral hemisphere region in dorsal  
22 view is larger, being *Vincelestes* higher than *Hadrocodium*. On the other hand,  
23 *Riograndia* present the lowest value of this ratio. Anyway, the non-mammaliaform  
24 cynodonts taxa in general presents similar values for this ratio, without a significant  
25 correlation, neither with the phylogenetic proximity to the mammals nor with the length  
26 of the skull.

27  
28  
29  
30  
31  
32  
33 However, it is interesting to note that among non-mammalian cynodonts there  
34 seems to be a trend of increase of the width of the cerebral hemispheres region  
35 according as the taxa are more closely related to mammals, indicated by the values of  
36 the aspect ratio (maximum width/length): *Massethognathus*, 0.35; *Probelesodon*, 0.32;  
37 *Probainognathus*, 0.57; *Therioherpeton*, 0.80; *Riograndia*, 0.84; *Brasilitherium*, 0.63;  
38 and *Hadrocodium*, 1.4 (the only one wider than long), while this ratio for the Theria  
39 *Vincelestes* is 0.59. Regarding to the non-mammaliaforms cynodont, it is worth noting  
40 the aspect ratio of the cerebral hemispheres region of *Brasilitherium*, lower than  
41 *Therioherpeton* and *Riograndia*, as well as *Probelesodon*, which present the lowest  
42 value among all taxa, although close to the value of *Massetognahtus*, do not fit in a  
43 phylogenetic sequence among mammaliamorphs more closely related to mammals.  
44 There is also a relationship between the aspect ratio of the cerebral hemispheres region  
45 and the skull length, so that the width is larger the smaller the skull, with the sole  
46 exception of *Riograndia*, in which the cerebral hemisphere region is relatively wider  
47 than *Therioherpeton*, but the specimen of the last taxa is smaller.

1  
2  
3 Moreover, a variation in the morphology of the cerebral hemispheres region can  
4 be represented by the ratio between the width measured near the posterior limit of the  
5 region and the width taken at half its length: *Massetognathus*, 1.24; *Probelesodon*,  
6 1.22; *Probainognathus*, 1.29; *Therioherpeton*, 1.59; *Riograndia*, 1.27; *Brasilitherium*,  
7 1.59; and *Hadrocodium*, 1.00; and *Vincelestes*, 0.72. Following a phylogenetic  
8 sequence, these ratios are similar among non-mammalian cynodonts and  
9 *Riograndia*, becomes higher in *Therioherpeton* and *Brasilitherium*, and then decays in  
10 *Hadrocodium* and – still more - in *Vincelestes*.

11  
12  
13  
14  
15  
16  
17  
18  
19 The cerebellar region

20  
21 The cerebellar region does not present a correlation with skull length or  
22 phylogenetic position regarding to the aspect ratio and related to the area of the  
23 endocast. Even so, a variation that may have some phylogenetic significance is observed  
24 with respect to the cerebellar width comparatively to the width of the cerebral  
25 hemispheres at the half of their length: *Massetognathus*, 1.56; *Probelesodon*, 1.43;  
26 *Probainognathus*, 1.16; *Therioherpeton*, 1.68; *Riograndia*, 1.45; *Brasilitherium*, 1.73;  
27 and *Hadrocodium*, 0.96; and *Vincelestes*, 0.71. Following a phylogenetic sequence, the  
28 ratios decay among non-mammalian cynodonts, then increase in *Therioherpeton*,  
29 *Riograndia* (the lowest value within non-mammalian mammalian forms) and  
30 *Brasilitherium*, and decays again in *Hadrocodium* and - more - in *Vincelestes*.

## 31 32 33 34 35 36 37 38 39 40 41 **DISCUSSION**

42 The study of the endocast of *Riograndia* reveals some important features. Within  
43 the characters commonly identified in the endocasts of the non-mammalian cynodonts, it  
44 is interesting to note the not so much conspicuous parafloccular casts. The vision between  
45 cerebral hemispheres is also less visible than in *Brasilitherium* but the aspect ratio of  
46 this region clearly indicates that it is not narrow as other non-mammalian cynodonts,  
47 so that the not deep median sulcus must be due to a single concavity in the internal  
48 surface of the frontal and parietal bones without a bony median ridge, but should not  
49 represent a primitive condition (the actual brain must have been divided in two cerebral  
50 hemispheres in this region).  
51  
52  
53  
54  
55  
56  
57  
58  
59  
60



1  
2  
3 Furthermore, It should be noted the marks suggested as vessel casts, since there  
4 is not mention of the transverse sinus for endocasts of non-mammaliaform cynodonts in  
5 previous works (Jerison 1973; Bonaparte, 1966; Quiroga, 1979, 1980a, b, c, 1984;  
6 Rodrigues et al. 2013), although it is the continuation of the prootic sinus, whose cast  
7 was identified in the endocast of *Brasilitherium* (Rodrigues et al., 2013). In addition,  
8 the ridge indentified as the transverse sinus presents a clear continuity with the filling of  
9 the unossified zone (dorsal region of the supraoccipital roofed by the parietal and  
10 perhaps partly the interparietal ) at the more central portion of the dorsal surface of the  
11 endocast. This mark in endocasts of non-mammalian cynodonts is interpreted as a  
12 cerebellar vermis cast (e.g. Kielan-Jaworowska et al., 2004). However, due to the  
13 continuity with a vascular mark, we interepretate the filling of the unossified zone  
14 (dorsal region of the supraoccipital roofed by the parietal and perhaps partly the  
15 interparietal) as the sagittal sinus, following (Rowe et al. 1995), although the vermis  
16 could have been present in *Riograndia*, covered by the vessel and extending posteriorly  
17 as central bulging visible on the dorsal surface of the cerebellar region, similar to the  
18 morphology described for the endocast of *Brasilitherium* (Rodrigues et al., 2013).  
19  
20  
21  
22  
23  
24  
25  
26  
27  
28  
29

30 Regarding to the quantititive approches, the EQs calculated can fit on a  
31 evolutionary sequence as it would be exepcted for *Riograndia* due to its phylogenetic  
32 position related to other taxa with EQs reported, taking into account the data of  
33 mammaliaform taxa, although the values are higher than the EQ calculated for  
34 *Brailitherium* by Rodrigues et al. (2013). This sequence can be corroborated by the  
35 most data of the non-mammaliamorph cyndonts, but the reported values for  
36 *Diademodon* reported by Jerison (1973) and, among the taxa studied by Quiroga (1979,  
37 1980a, b, c, 1984), at least the EQ of *Massetognathus*, disregarding all EQs calculated  
38 from one of the equations that the last author used to estimate body mass. These EQs  
39 appears overestimated, not only by the phylogenetic relationship of the taxa, but by the  
40 morphology observed, as noted by Rodrigues et al. (2013, see FIG. 10). We can artibute  
41 these overestimated EQs due to inaccuracy in endocast volume measurement  
42 (considering that the works used natural endocasts, extracted form the skull, although  
43 posterior studies can use CT scan), as well as the body mass estimates from The mass  
44 estimates from little or a single factor (usually skull length), for specimens of different  
45 size (and hence, body proportions). The equation that we used to estimate the body mass  
46  
47  
48  
49  
50  
51  
52  
53  
54  
55  
56  
57  
58  
59  
60

1  
2  
3 of *Riograndia* seems to be more realistic, since the equation is used for mammaliaforms  
4 and based on insectivores, being all taxa of small size and similar body design.  
5  
6

7  
8 Anyway, in addition to the finding of relative increase in overall brain size, we  
9 consider it important to seek to identify which structures are responsible for volumetric  
10 growth in general and how these variables can be related. In this sense, in spite of the  
11 limitations of sampling, as well as possible inaccuracies of measurements from  
12 photographs of other works and the restriction itself because only the surface dorsally  
13 exposed in 2D is being evaluated, at least the three main regions (i.e. olfactory bulbs,  
14 cerebral hemispheres and cerebellum) dorsally visible could be studied comparatively  
15 with respect to the relative size. In fact, the methodological limitations do not seem to  
16 us greater than the inaccuracies of volumetric studies with extinct taxa and mass  
17 estimates. Due to the covariation of these structures within the taxa, several different  
18 ratios were calculated in order to isolate variables, and the results obtained must indicate  
19 some neurological adaptations along the evolution of the lineage of the cynodonts, as  
20 pointed out below.  
21  
22  
23  
24  
25  
26  
27  
28

29  
30 Thus, we can suggest a sequence of changes in cynodonts successively more  
31 closely related to mammals, from the primitive pattern represented by *Massetognathus*  
32 and *Probelesodon*. The changes suggested evolve basically increasing of regions of the  
33 endocast in relation to both the whole endocast and the skull:  
34  
35

36  
37 1) The increase in the relative size of the olfactory bulbs among non-mammalian  
38 cynodonts - a continuous increase, but more pronounced within Prozostodontia;  
39

40  
41 2) The increase in the relative width of the cerebral hemispheres at the posterior  
42 portion – a continuous increase from *Probainognathus* to mammaliaformes;  
43

44  
45 3) The increase of the relative width of the whole cerebral hemispheres region -  
46 mainly from Prozostodontia;  
47

48  
49 4) The increase of the width of the cerebellar region related to the skull (not  
50 necessarily relative to the whole endocast because of the growth of the regions  
51 mentioned above) - from Prozostodontia.  
52  
53  
54  
55

56  
57 Thus, taking into account the different ratios showed in the Table 3, we can  
58 suggest the trend of increase of the olfactory bulbs, being the apex represented by  
59  
60

1  
2  
3 *Brasilitherium*. The value for the relative area of the dorsal surface of this region, higher  
4 in *Probelesodon* than *Probainognathus*, could be explained by the fact that the width of  
5 the cerebral hemispheres region is increased from *Probainognathus* to other taxa more  
6 closely related to mammaliaforms, as indicated by the aspect ratio of the cerebral  
7 hemispheres region, changing from 0.35 in *Massetognathus* and 0.33 *Probelesodon* to  
8 0.57 in *Probainognathus*, and so 0.80, in *Therioherpeton* and 0.84 in *Riograndia*  
9 *Brasilitherium*, 0.63. Indeed, it is clear the increase of the width of the cerebral  
10 hemispheres region, from a narrow and apparently tubular morphology, without division  
11 in two hemispheres on the endocast, the condition represented by *Massetognathus* and  
12 *Probelesodon* (although, in the last taxon, already appears the increase in the size of the  
13 bulbs) to a morphology with clear divided cerebral hemispheres, and increasing the  
14 width as the taxa are closer to mammals.

15  
16  
17  
18  
19  
20  
21  
22  
23  
24 Still regarding to the aspect ratio of the cerebral hemispheres, it is interesting the  
25 value of *Brasilitherium*, the lowest among non-mammaliaform mammaliaforms,  
26 indicating elongated cerebral hemispheres. However, this taxon, in addition to having  
27 higher values than the non-mammaliaform cynodonts, presents the lowest values  
28 related to the dorsal exposition of the cerebellar region, which can suggest a posterior  
29 elongation covering the cerebellum and not a condition near to the narrow brains of the  
30 non-mammaliaform cynodonts. Moreover, *Brasilitherium* presents a conspicuous  
31 division between the cerebral hemispheres (see Rodrigues et al., 2013) and the clear  
32 increase of the width of the posterior portion of this region. In this regard, the ratio  
33 between the width of the cerebral hemispheres region near to the posterior limit, and the  
34 width of the region at the half of the length, indicate values about 1.2 for  
35 *Massetognathus* and *Probelesodon*, increasing to near of 1.3 in *Probainognathus* and  
36 *Riograndia*, and reaching about 1.6 in *Therioherpeton* and *Brasilitherium*. Within the  
37 mammaliaforms, this ratio is 1.0 in *Hadrocodium*, evidencing a relative growth in width  
38 at the median portion of the cerebral hemispheres, until it exceeds the width of the  
39 posterior limit in *Vincelestes* (0.7).

40  
41  
42  
43  
44  
45  
46  
47  
48  
49  
50  
51 In view of the foregoing, we can suggest an evolutionary sequence from the  
52 narrow brains the non-mammaliaform cynodonts with more basal position related to  
53 mammals, starting by a gradual increase of the olfactory bulbs, which must be associated  
54 to the changes in the nasal cavity evolving the closure and posterior extension of the  
55 ossified secondary palate, as well as the complex of the nasal turbinates (e.g. Hillenius,  
56  
57  
58  
59  
60

1  
2  
3 1994; Kielan-Jaworowska et al. 2004; Ruf et al 2014). These changes, in turn, are  
4 associated to the breathing with an endothermic metabolism (e.g. Hillenius, 1992,  
5 1994), at the same time that they enable an improvement in olfaction sense. Thus, the  
6 selective pressure to improve the olfaction seems to be an important factor in the  
7 beginning of the evolution of the mammalian brain, being this sense, as mentioned by  
8 Jerison (1973), a very significant feature to the nocturnal habits of the small sized  
9 animals (i.e. non-mammalian mammaliamorphs).

10  
11  
12  
13  
14  
15 This study of *Riograndia*, as well as the taxa using for comparison, corroborate  
16 this trend, being the maximum development of the olfactory bulbs related to the  
17 endocast represented by *Brasilitherium*, just the taxon that appears as the sister-group of  
18 mammaliaforms in phylogentic analysis (e.g. Bonaparte et al 2003; Martinelli &  
19 Rougier 2007; Abdala 2007; Liu & Olsen, 2010.). Among mammliaforms, the relative  
20 size of olfactory bulbs seems to decay, which must be associated to the enlargement of  
21 the cerebral hemispheres, which corresponds to the first and second of the three  
22 “pulses” indicated for Rowe et al. (2011) in the evolution of the mammal brain,  
23 represented by *Morganucodon* and *Hadrocodium*, respectively.

24  
25  
26  
27  
28  
29  
30  
31 As already hypothesized by Rodrigues et al (2013), it seems to have been a  
32 neurological evolution of the mammlian lineage starting by the improvement of the  
33 sensory receptor system (adaptations on the nasal cavity) and increase of the primary  
34 processing strucures (i.e. olfactory bulbs), leading to further development of the  
35 “superior” structures of the neurological system, for sensorial processing and integration  
36 in the brain (i.e. cerebral hemispheres). After, following the sequence indicated by  
37 Rowe et al. (2011), the third pulse is represented in the origin mammalian crown-group,  
38 associated to other adaptations of olfactory reception: the ossified ethmoturbinals, a  
39 cribriform plate and a rigid support in the nasal cavity to the olfactory epithelium  
40 receptor (whose genes exceed by about one order of magnitude the amount existing in  
41 the genome of most other vertebrates; Niimura, 2009).

42  
43  
44  
45  
46  
47  
48  
49 Regarding the evolution of the cerebral hemispheres, we can suggest an initial  
50 increase in width at the posterior portion, possibly associated to the increease in width  
51 of the cerebellum. This trend can be not the same indicated by Kemp (2009), regarding  
52 to the size of the cerebellum, which is represented already by cynodonts of basal  
53 position related mammalimorphs. This initial cerebellar development mentioned by  
54 Kemp (2009) can be reflect the improvement of the neuromuscular control associated to  
55  
56  
57  
58  
59  
60

1  
2  
3 a complex occluding posterior teeth, jaw musculature to a bite forceful and precise,  
4 more upright hindlimbs and mobility of the shoulder girdle. In turn, the increase of the  
5 cerebellar width among mammaliamorphs, mainly in non-mammalian mammaliforms,  
6 can be associated to the adaptations of the auditory system, reflected by the  
7 development of the cochlea and the petrosal promontorium, at least from *Brasilitherium*  
8 (Rodrigues et al. 2013).  
9

10  
11  
12  
13 Indeed, the reduced number of specimens compared does not allow an accurate  
14 distinction between phylogenetic influence and some allometric relation with skull size,  
15 which would require studies involving ontogenetic series. It would be also interesting  
16 because there is some correlation between the closer phylogenetic relationship with  
17 mammals, and the small body size, since the neurological and sensorial adaptations of  
18 the mammalian lineage among non-mammalian cynodonts are also concomitant with the  
19 evolutionary process of the miniaturization in Mesozoic cynodonts.  
20  
21  
22  
23  
24  
25

## 26 **ACKNOWLEDGEMENTS**

27  
28 Thomas G. Davies for ct assistance at Bristol University. The scan was obtained with  
29 support of NERC (Natural Environment Research Council) grant number  
30 NE/K01496X/1 to ER. This work is supported by the Conselho Nacional de  
31 Desenvolvimento Científico e Tecnológico (CNPq).  
32  
33  
34  
35

## 36 **REFERENCES**

- 37  
38 Abdala, F. 2007. Redescription of *Platycraniellus elegans* (Therapsida, Cynodontia)  
39 from the Lower Triassic of South Africa, and the cladistic relationships of  
40 eutheriodonts. *Palaeontology* 50(3): 591–618.  
41  
42  
43  
44 Abdala, F.; Giannini, N. P. 2000. Gomphodont cynodonts of the Chañares Formation:  
45 the analysis of an ontogenetic sequence. *Journal of Vertebrate Paleontology* 20:  
46 501–506.  
47  
48  
49 Bauchot, R.; Stephan H. 1967. Encephales et moulages endocraniens de quelque  
50 insectivores et primates actuels. *Colloques Internationaux du Centre National de la*  
51 *Recherche Scientifique* 163: 575–587.  
52  
53  
54  
55 Bonaparte, J.F. 1966. Sobre las cavidades cerebral, nasal y otras estructuras del craneo  
56 de *Exaeretodon* sp. (Cynodontia-Traversodontidae). *Acta Geologica Lilloana* 8: 5–  
57 11.  
58  
59  
60

- 1  
2  
3 Bonaparte, J. F.; J. Ferigolo; A. M. Ribeiro. 2001. A primitive Late Triassic “ictidosaur”  
4 from Rio Grande do Sul, Brazil. *Palaeontology* 44: 623–635.  
5  
6  
7 Bonaparte, J.F.; Martinelli, A.G.; Schultz, C.L.; Rupert, R. 2003. The sister group of  
8 mammals: small cynodonts from the late Triassic of southern Brazil. *Revista*  
9 *Brasileira de Paleontologia*, 5: 5-27.  
10  
11  
12 Butler, A.B., Hodos, W. 1996. *Comparative Vertebrate Neuroanatomy: Evolution and*  
13 *Adaptation*. New York: Wiley-Liss.  
14  
15  
16 Colbert, M.W., Racicot, R.; Rowe, T. 2005. Anatomy of the cranial endocast of the  
17 bottlenose dolphin *Tursiops truncatus*, based on HRXCT. *Journal of Mammalian*  
18 *Evolution* 12: 195–207.  
19  
20  
21 Dom, R., B.L. Fisher, and G.F. Martin. 1970. The venous system of the head and neck  
22 of the opossum (*Didelphis virginiana*). *Journal of Morphology* 132: 487–496.  
23  
24  
25 Edinger, T. 1964. Midbrain exposure and overlap in mammals. *American Zoologist* 4:  
26 5–19.  
27  
28  
29 Eisenberg, J.F. 1981. *The Mammalian Radiations*. Chicago: University of Chicago.  
30  
31 Eisenberg, J.F., and D.E. Wilson. 1978. Relative brain size and feeding strategies in the  
32 Chiroptera. *Evolution* 32: 740–751. Eisenberg, J.F., and D.E. Wilson. 1981.  
33 Relative brain size and demographic strategies in *Didelphis marsupialis*. *American*  
34 *Naturalist* 118: 1–15.  
35  
36  
37  
38 Gingerich, P.D.; B.H. Smith. 1984. Allometric scaling in the dentition of primates and  
39 insectivores. In *Size and Scaling in Primate Biology*, ed. W.L. Jungers, 257–272.  
40 New York: Plenum Press.  
41  
42  
43 Hillenius, W.J. 1992. The evolution of nasal turbinates and mammalian endothermy.  
44 *Paleobiology* 18: 17-29  
45  
46  
47 Hillenius, W.J. 1994. Turbinates in therapsids: evidence for Late Permian origins of  
48 mammalian endothermy. *Evolution*, 48: 207-229.  
49  
50  
51 Hopson, J.A. 1964. The braincase of the advanced mammal-like reptile *Bienotherium*.  
52 *Postilla*, 87: 1-30.  
53  
54  
55 Hopson, J.A. 1979. Paleoneurology. In *Biology of the Reptilia, Volume 9, Neurology A*,  
56 ed. C. Gans, R.G. Northcutt, and P. Ulinski, 39–146. London: Academic Press.  
57  
58  
59  
60

- 1  
2  
3 Hopson, J.A., and Kitching, J.W. 2001. A probainognathian cynodont from South  
4 Africa and the phylogeny of nonmammalian cynodonts. In *Studies in Organismic  
5 and Evolutionary Biology in Honor of Alfred W. Crompton—Bulletin of Museum  
6 of Comparative Zoology*, vol. 156, eds. F.A. Jenkins, M.D. Shapiro, and T.  
7 Owerkowicz, 5–35.  
8  
9  
10  
11 Horn, B.L.D.; Melo, T.M.; Schultz, C.L.; Philipp, R.P.; Kloss, H.P.; Goldberg, K. 2014.  
12 A new third-order sequence stratigraphic framework applied to the Triassic of the  
13 Parana Basin, Rio Grande do Sul, Brazil, based on structural, stratigraphic and  
14 paleontological data. *Journal of South American Earth Sciences*, 55: 123-132.  
15  
16  
17  
18 Jerison, H.J. 1973. *Evolution of the Brain and Intelligence*. New York: Academic Press.  
19  
20  
21 Jerison, H.J. 1991. Fossil brains and the evolution of the neocortex. In *The Neocortex:  
22 Ontogeny and Phylogeny*. NATO Advanced Science Institutes Series A: Life  
23 Sciences vol. 200, eds. B.L. Finlay, G. Innocenti, and H. Scheich. New York:  
24 Plenum Press.  
25  
26  
27  
28 Kemp, T.S. 1979. The primitive cynodont *Procynosuchus*: structure, function, and  
29 evolution of the postcranial skeleton. *Philosophical Transactions of the Royal  
30 Society of London. Series B* 288: 217–258.  
31  
32  
33  
34 Kemp, T.S. 2009. The endocranial cavity of a nonmammalian cynodonts *Chiniquodon  
35 theotenicus* and its implications for the origin of the mammalian brain. *Journal of  
36 Vertebrate Paleontology* 29(4): 1188–1198.  
37  
38  
39 Kielan-Jaworowska, Z. 1983. Multituberculate endocranial casts. *Palaeovertebrata* 13:  
40 1–12.  
41  
42  
43 Kielan-Jaworowska, Z. 1984. Evolution of the therian mammals in the late Cretaceous  
44 of Asia. Part VI. Endocranial casts of eutherian mammals. *Palaeontologia Polonica*  
45 46: 157–171.  
46  
47  
48 Kielan-Jaworowska, Z. 1986. Brain evolution in Mesozoic mammals. In *Vertebrates,  
49 Phylogeny, and Philosophy*. Contributions to Geology, University of Wyoming,  
50 Special Paper 3, eds. K.M. Flanagan, and J.A. Lillegraven, 21–34.  
51  
52  
53  
54  
55  
56 Kielan-Jaworowska, Z., R.L. Cifelli, and Z.-X. Luo. 2004. *Mammals from the Age of  
57 Dinosaurs: Origin, Evolution, and Structure*. New York: Columbia University Press.  
58  
59  
60

- 1  
2  
3 Kielan-Jaworowska, Z., and T.E. Lancaster. 2004. A new reconstruction of  
4 multituberculate endocranial casts and encephalization quotient of *Kryptobaatar*.  
5 Acta Palaeontologica Polonica 49: 177–188.  
6  
7  
8 Krause, D.W., and Z. Kielan-Jaworowska. 1993. The endocranial cast and  
9 encephalization quotient of *Ptilodus* (Multituberculata, Mammalia).  
10 Palaeovertebrata 22: 99–112.  
11  
12  
13 Liu, J., and P. Olsen. 2010. The phylogenetic relationships of Eucynodontia (Amniota:  
14 Synapsida). Journal of Mammalian Evolution 17: 151–176.  
15  
16  
17 Loo, Y.T. 1930. The forebrain of the opossum, *Didelphis virginiana*. Journal of  
18 Comparative Neurology 51: 13–64.  
19  
20  
21 Luo, Z.-X. 1994. Sister-group relationships of mammals and transformations of  
22 diagnostic mammalian characters; In: FRASER, N. C.; SUES, H. D. (eds.), In the  
23 Shadow of the Dinosaurs: Early Mesozoic Tetrapods. New York: Cambridge  
24 University Press, p. 98-128.  
25  
26  
27  
28 Luo, Z.-X., A.W. Crompton, and A.-L. Sun. 2001. A new mammaliaform from the early  
29 Jurassic and evolution of mammalian characteristics. Science 292: 1535–1540.  
30  
31  
32 Luo, Z.-X., Z. Kielan-Jaworowska, and R.L. Cifelli. 2002. In quest for a phylogeny of  
33 Mesozoic mammals. Acta Palaeontologica Polonica 47: 1–78.  
34  
35  
36 Macrini, T. E. 2006. The evolution of endocranial space in mammals and non-  
37 mammalian cynodonts. Ph.D. dissertation. The University of Texas at Austin, 278  
38 pp.  
39  
40  
41 Macrini, T.E., T. Rowe, and M. Archer. 2006. Description of a cranial endocast from a  
42 fossil platypus, *Obdurodon dicksoni* (Monotremata, Ornithorhynchidae), and the  
43 relevance of endocranial characters to monotreme monophyly. Journal of  
44 Morphology 267: 1000–1015.  
45  
46  
47  
48 Macrini, T.E., C. Muizon, R.L. Cifelli, and T. Rowe. 2007a. Digital cranial endocast of  
49 *Pucadelphys andinus*, a Paleocene metatherian. Journal of Vertebrate Paleontology  
50 27: 99–107.  
51  
52  
53  
54 Macrini, T.E., G.W. Rougier, and T. Rowe. 2007b. Description of a cranial endocast  
55 from the fossil mammal *Vincelestes neuquenianus* (Theriiformes) and its relevance  
56  
57  
58  
59  
60



- 1  
2  
3 to the evolution of endocranial characters in therians. *The Anatomical record*  
4 290(7): 875–892.  
5  
6  
7 Maier, W. 1987. The ontogenetic development of the orbitotemporal region of the skull  
8 of *Monodelphis domestica* (Didelphidae, Marsupialia), and the problem of the  
9 mammalian alisphenoid. *Mammalia Depicta* 13: 71–90.  
10  
11  
12 Martinelli, A. G. & G. W. Rougier. 2007. On *Chalimnia musteloides* Bonaparte  
13 (Cynodontia, Tritheledontidae) and the phylogeny of the Ictidosauria. *Journal of*  
14 *Vertebrate Paleontology* 27: 442–460.  
15  
16  
17 Meisami E, Bhatnagar KP. 1998. Structure and diversity in mammalian accessory  
18 olfactory bulb. *Microsc Res Tech* 43:476–499.  
19  
20  
21 Mauk, M. D., J. F. Medina, W. L. Nores, and T. Ohyama. 2000. Cerebellar function:  
22 coordination, learning or timing? *Current biology* 10: R522–R525.  
23  
24  
25 Negus V. 1958. The comparative anatomy and physiology of the nose and paranasal  
26 sinuses. London: E&S Livingstone Ltd. 402 p.  
27  
28  
29 Niimura, Y. 2009. On the origin and evolution of vertebrate olfactory receptor genes:  
30 comparative genome analysis among 23 chordate species. *Genome Biology and*  
31 *Evolution* 1: 34–44.  
32  
33  
34 Novacek, M.J. 1993. Mammalian phylogeny: morphology and molecules. *Trends in*  
35 *Ecology and Evolution* 8(9): 339–340.  
36  
37  
38 Oliveira, T. V., MB. Soares & C. L. Schultz. 2010. *Trycidocynodon riograndensis* gen.  
39 nov. et sp. nov. (Eucynodontia), a new cynodont from the Brazilian Upper Triassic  
40 (Santa Maria Formation). *Zootaxa* 2382: 1–71.  
41  
42  
43 Pirlot P, Nelson J. 1978. Volumetric analysis of monotreme brains. *Aust Zool* 20:171–  
44 179.  
45  
46  
47 Presley, R. 1980. The braincase in Recent and Mesozoic therapsids. *Mémoires, Société*  
48 *Géologique de France N.S.*, 139: 159–162.  
49  
50  
51 Quiroga, J.C. 1979. The brain of two mammal-like reptiles (Cynodontia- Therapsida).  
52 *Journal für Hirnforschung* 20: 341–350.  
53  
54  
55  
56  
57  
58  
59  
60

- 1  
2  
3 Quiroga, J.C. 1980a. Sobre un molde endocraneano del cinodonte *Probainognathus*  
4 *jenseni* Romer, 1970 (Reptilia, Therapsida), de la Formación Ischichuca (Triasico  
5 Medio), La Rioja, Argentina. *Ameghiniana* 17: 181–190.  
6  
7  
8  
9 Quiroga, J.C. 1980b. The brain of the mammal-like reptile *Probainognathus jenseni*  
10 (Therapsida, Cynodontia). A correlative paleo-neoneurological approach to the  
11 neocortex at the reptilemammal transition. *Journal für Hirnforschung* 21: 299–336.  
12  
13 Quiroga, J.C. 1980c. Descripción de los moldes endocraneanos de dos cinodontes  
14 (Reptilia–Therapsida) de Los Chañares–Triasico medio–de la Provincia de La  
15 Rioja (Argentina). Notas sobre al sistema vascular intracraneano y relaciones con  
16 los moldes dde otros Cinodontes en función de la morfología de los más antiguos  
17 moldes mamalianos conocidos. In II Congreso Argentino de Paleontología y  
18 Bioestratigrafía y I Congreso Latinoamericano de Paleontología. Actas, 103–122.  
19 Buenos Aires.  
20  
21  
22  
23  
24  
25  
26 Quiroga, J.C. 1984. The endocranial cast of the advanced mammallike reptile  
27 *Therioherpeton cargini* (Therapsida- Cynodontia) from the Middle Triassic of  
28 Brazil. *Journal für Hirnforschung* 25: 285–290.  
29  
30  
31  
32 Rodrigues PG, Ruf I, Schultz CL 2013. Study of a digital cranial endocast of the non-  
33 mammaliaform cynodont *Brasilitherium riograndensis* (Later Triassic, Brazil) and  
34 its relevance to the evolution of the mammalian brain. *Paläontologische Zeitschrift*  
35 88: 329-352.  
36  
37  
38  
39 Roth, J.J., Roth, E.C., and N. Hotton III. 1986. The parietal foramen eye: their function  
40 and fate in therapsids. In *The Ecology and Biology of Mammal-like Reptiles*, eds.  
41 N. Hotton III, P.B. Maclean, J.J. Roth, and E.C. Roth, 173–184. Washington, DC:  
42 Smithsonian Institute Press.  
43  
44  
45  
46 Rougier, G.W., and J.R. Wible. 2006. Major changes in the ear region and basicranium  
47 of early mammals. In *Amniote Paleobiology: Phylogenetic and Functional*  
48 *Perspectives on the Evolution of Mammals, Birds and Reptiles*, eds. M. Carrano,  
49 T.J. Gaudin, R. Blob, and J.R. Wible, 269–311. Chicago: University of Chicago  
50 Press.  
51  
52  
53  
54  
55 Rowe, T. 1996. Coevolution of the mammalian middle ear and neocortex. *Science* 273:  
56 651–654.  
57  
58  
59  
60

- 1  
2  
3 Rowe, T., W. Carlson, and W. Bortorff. 1995. *Thrinaxodon*: Digital Atlas of the Skull.  
4 CD-ROM (Second Edition for Windows and Macintosh platforms. University of  
5 Texas Press, Austen, Texas pp.  
6  
7  
8  
9 Rowe, T.B., T.P. Eiting, T.E. Macrini, and R.A. Ketcham. 2005. Organization of the  
10 olfactory and respiratory skeleton in the nose of the gray short-tailed opossum  
11 *Monodelphis domestica*. Journal of Mammalian Evolution 12: 303–336.  
12  
13  
14 Rowe, T.B., T.E. Macrini, and Z.-X. Luo. 2011. Fossil evidence on origin of the  
15 mammalian brain. Science 332: 955–957.  
16  
17  
18 Ruff I, Maier W, Rodrigues PG, Schultz CL. 2014. Nasal anatomy of the non-  
19 mammaliaform cynodont *Brasilitherium riograndensis* (Eucynodontia, Therapsida)  
20 reveals new insight into mammalian evolution. Anat Rec. 297(11): 2018–2030.  
21  
22  
23 Sánchez-Villagra, M.R. 2002. The cerebellar paraflocculus and the subarcuate fossa in  
24 *Monodelphis domestica* and other marsupial mammals: ontogeny and phylogeny of  
25 a brain-skull interaction. Acta Theriologica 47: 1–14.  
26  
27  
28  
29 Silcox, M.T., C.K. Dalmyn, A. Hrenchuk, J.I. Bloch, D.M. Boyer, and P. Houde. 2011.  
30 Endocranial morphology of *Labidolemur kayi* (Apatemyidae, Apatotheria) and its  
31 relevance to the study of brain evolution in Euarchontoglires. Journal of Vertebrate  
32 Paleontology 31: 1314–1325.  
33  
34  
35  
36 Soares, M. B., C. L. Schultz & B. L. D. Horn. 2011. New information on *Riograndia*  
37 *guaibensis* Bonaparte, Ferigolo & Ribeiro, 2001 (Eucynodontia, Tritheledontidae)  
38 from the Late Triassic of southern Brazil: anatomical and biostratigraphic  
39 implications. Anais da Academia Brasileira de Ciências 83: 329– 354.  
40  
41  
42  
43 Sues, H-D. 1986. The skull and dentition of two tritylodontid synapsids from the Lower  
44 Jurassic of Western North America. Bulletin of the Museum of Comparative  
45 Zoology, 151: 217-268.  
46  
47  
48  
49 Starck, D. 1979. Vergleichende Anatomie der Wirbeltiere auf evolutionsbiologischer  
50 Grundlage, Bd. 2, XII. Berlin: Springer.  
51  
52  
53 Watson, D.M.S. 1913. Further notes on the skull, brain, and organs of special sense of  
54 *Diademodon*. The Annals and Magazine of Natural History, Series 8(12): 217–228.  
55  
56  
57 Wible, J.R.; Hopson, J.A. 1995. Homologies of the prootic canal in mammals and non-  
58 mammalian cynodonts. Journal of Vertebrate Paleontology, 15 : 331-356.  
59  
60

1  
2  
3 Zerfass, H., E. L. Lavina, C. L. Schultz, A. J. V. Garcia, U. F. Faccini & Jr. F. Chemale.  
4 2003. Sequence stratigraphy of continental Triassic strata of Southernmost Brazil: a  
5 contribution to Southwestern Gondwana palaeogeography and palaeoclimate.  
6 Sedimentary Geology 161: 85–105.  
7  
8  
9  
10  
11  
12  
13  
14  
15  
16  
17  
18  
19  
20  
21  
22  
23  
24  
25  
26  
27  
28  
29  
30  
31  
32  
33  
34  
35  
36  
37  
38  
39  
40  
41  
42  
43  
44  
45  
46  
47  
48  
49  
50  
51  
52  
53  
54  
55  
56  
57  
58  
59  
60

For Peer Review Only

---

|    |  |                 |
|----|--|-----------------|
| 1  |  |                 |
| 2  |  |                 |
| 3  | Length of the endocast, measured from the anterior limit of the dorsal         |                 |
| 4  | surface of the olfactory bulb to the foramen magnum                            | 17.67 mm        |
| 5  |  |                 |
| 6  | Maximum width  | 6.88 mm         |
| 7  |  |                 |
| 8  | Maximum height, measured from the ventral limit of the hypophyseal cast        |                 |
| 9  | to the dorsal surface above it   | 8.71 mm         |
| 10 |  |                 |
| 11 | Maximum height, corresponding to the distance between the ventral limit of     |                 |
| 12 | the hypophyseal cast and the most dorsal point of the olfactory bulb casts)    | 10.08 mm        |
| 13 |  |                 |
| 14 |  | 445.44          |
| 15 | Volume of the whole endocast   | mm <sup>3</sup> |
| 16 |  |                 |
| 17 | Volume of the endocast with the rocky filling of the orbital vacuity digitally | 404.20          |
| 18 | removed  | mm <sup>3</sup> |
| 19 |  |                 |
| 20 | Length of the dorsal surface of the two olfactory bulb casts                   | 7.10 mm         |
| 21 |  |                 |
| 22 | Maximum width of the olfactory bulb casts together                             | 4.12 mm         |
| 23 |  |                 |
| 24 |  | 79.49           |
| 25 | Estimated volume for the region of the olfactory bulb region *                 | mm <sup>3</sup> |
| 26 |  |                 |
| 27 | Width of the endocast at the limit between the olfactory bulb casts and        | 3.90 mm         |
| 28 | cerebral hemispheres region  |                 |
| 29 |  |                 |
| 30 | Length of the dorsal surface of the region of the cerebral hemisphere casts    | 7.53 mm         |
| 31 |  |                 |
| 32 | Maximum width of the dorsal surface at the region of the cerebral              |                 |
| 33 | hemisphere casts   | 5.26 mm         |
| 34 |  |                 |
| 35 | Anteroposterior length of the dorsal surface (slope) of the cerebellar region  | 4.68 mm         |
| 36 |  |                 |
| 37 | Anteroposterior length of the cerebellar region taking a horizontal line       | 1.90 mm         |
| 38 |  |                 |
| 39 | Width of the cerebellar region (between the parafloccular casts)               | 6.20 mm         |
| 40 |  |                 |
| 41 | Distance between the apex of the left parafloccular cast and the adjacent      |                 |
| 42 | lateral surface  | 0.72 mm         |
| 43 |  |                 |
| 44 | Distance between the apex of the right parafloccular cast and the adjacent     |                 |
| 45 | lateral surface  | 0.74 mm         |
| 46 |  |                 |
| 47 | Length of the ventral opening of the cavum epiptericum (left side)             | 5 mm            |
| 48 |  |                 |
| 49 |  |                 |
| 50 |  |                 |
| 51 |  |                 |
| 52 |  |                 |
| 53 |  |                 |
| 54 |  |                 |
| 55 |  |                 |
| 56 |  |                 |
| 57 |  |                 |
| 58 |  |                 |
| 59 |  |                 |
| 60 |  |                 |

---

\*Values based on the ventral contour and anterior limit estimated for the olfactory bulbs by removing the infilling of the orbital vacuity in order to make the ventral contour becomes similar to the dorsal contour.

For Peer Review Only

| <b>Taxon</b>           | <b>EQ<sup>1</sup></b> | <b>EQ<sup>2</sup></b> | <b>Source</b>                          |
|------------------------|-----------------------|-----------------------|--|
| <i>Thrinaxodon</i> ,   | 0.1                   |                       | Jerison (1973)                         |
| <i>Diademodon</i>      | 0.21                  |                       |  |
|                        | 0.14                  |                       | Quiroga (1980b)                        |
| <i>Massetognathus</i>  | 0.15; 0.22            |                       | Quiroga (1979, 1980b)                  |
| <i>Exaeretodon</i>     | 0.10; 0.15            |                       | Quiroga (1980b)                        |
| <i>Probolesodon</i>    | 0.13; 0.18            |                       | Quiroga (1979, 1980b)                  |
| <i>Probainognathus</i> | 0.12; 0.17            |                       | Quiroga (1980a, b)                     |
| <i>Riograndia</i>      | 0.22                  | 0.33                  | This study                             |
|                        | 0.20                  | 0.30                  |  |
| <i>Brasilitherium</i>  | 0.15                  | 0.22                  | Rodrigues et al. (2013XX)              |
| <i>Morganucodon</i>    |                       | 0.32                  | Rowe et al. (2011)                     |
| <i>Hadrocodium</i>     |                       | 0.49                  |  |
| <i>Obdurodon</i>       |                       | 1.00                  | Macrini et al. (2007a)                 |
| living monotremes      |                       | 0.75-0.89             |  |
| <i>Triconodon</i>      |                       | 0.49                  | Kielan-Jaworowska (1983)               |
| <i>Chulsanbaatar</i>   |                       | 0.55                  |  |
| <i>Kryptobaatar</i>    |                       | 0.71                  | Kielan-Jaworowska and Lancaster (2004) |
| <i>Ptilodus</i>        |                       | 0.49                  | Kielan-Jaworowska (1983)               |
| <i>Vincelestes</i>     |                       | 0.37                  | Macrini et al. (2007b)                 |
| <i>Kennalestes</i>     |                       | 0.36                  | Kielan-Jaworowska (1984)               |
| <i>Asioryctes</i>      |                       | 0.56                  |  |
| <i>Zambdalestes</i>    |                       | 0.7                   |  |
| didelphids             |                       | 0.5-1.09              | Eisenberg and Wilson (1981)            |

| Taxa (skull length)            | length/skull length |       |       |       | area/ endocast area |       |       | maximum width / length |       |       |       | width/CH mid width |          |       |
|--------------------------------|---------------------|-------|-------|-------|---------------------|-------|-------|------------------------|-------|-------|-------|--------------------|----------|-------|
|                                | E                   | OB    | CH    | CR    | OB                  | CH    | CR    | E                      | OB    | CH    | CR    | OB                 | CH post. | CR    |
| <i>Vincelestes</i> (63 mm)     | 0,545               | 0,169 | 0,322 | 0,061 | 0,194               | 0,667 | 0,139 | 0,474                  | 0,836 | 0,589 | 3,034 | 0,546              | 0,727    | 0,716 |
| <i>Hadrocodium</i> (12 mm)     | 0,627               | 0,219 | 0,322 | 0,096 | 0,230               | 0,603 | 0,167 | 0,768                  | 1,094 | 1,488 | 4,504 | 0,492              | 1,001    | 0,958 |
| <i>Brasilitherium</i> (38 mm)  | 0,450               | 0,182 | 0,265 | 0,038 | 0,352               | 0,563 | 0,085 | 0,402                  | 0,625 | 0,626 | 4,738 | 1,048              | 1,585    | 1,730 |
| <i>Riograndia</i> (35 mm)      | 0,443               | 0,169 | 0,188 | 0,082 | 0,300               | 0,443 | 0,256 | 0,405                  | 0,668 | 0,839 | 2,188 | 0,912              | 1,274    | 1,448 |
| <i>Therioherpeton</i> (31 mm)  | 0,680               | 0,283 | 0,346 | 0,059 | 0,336               | 0,538 | 0,126 | 0,429                  | 0,807 | 0,797 | 4,927 | 1,317              | 1,593    | 1,682 |
| <i>Probainognathus</i> (65 mm) | 0,583               | 0,158 | 0,323 | 0,131 | 0,222               | 0,556 | 0,223 | 0,316                  | 0,793 | 0,570 | 1,267 | 0,899              | 1,285    | 1,161 |
| <i>Probelesodon</i> (120 mm)   | 0,406               | 0,127 | 0,267 | 0,034 | 0,287               | 0,576 | 0,137 | 0,223                  | 0,575 | 0,325 | 3,166 | 1,073              | 1,221    | 1,430 |
| <i>Massetognathus</i> (95 mm)  | 0,517               | 0,125 | 0,303 | 0,109 | 0,217               | 0,570 | 0,213 | 0,260                  | 0,724 | 0,353 | 1,235 | 1,048              | 1,237    | 1,558 |



1  
2  
3  
4  
5  
6  
7  
8  
9  
10  
11  
12  
13  
14  
15  
16  
17  
18  
19  
20  
21  
22  
23  
24  
25  
26  
27  
28  
29  
30  
31  
32  
33  
34  
35  
36  
37  
38  
39  
40  
41  
42  
43  
44  
45  
46  
47  
48  
49  
50  
51  
52  
53  
54  
55  
56  
57  
58  
59  
60

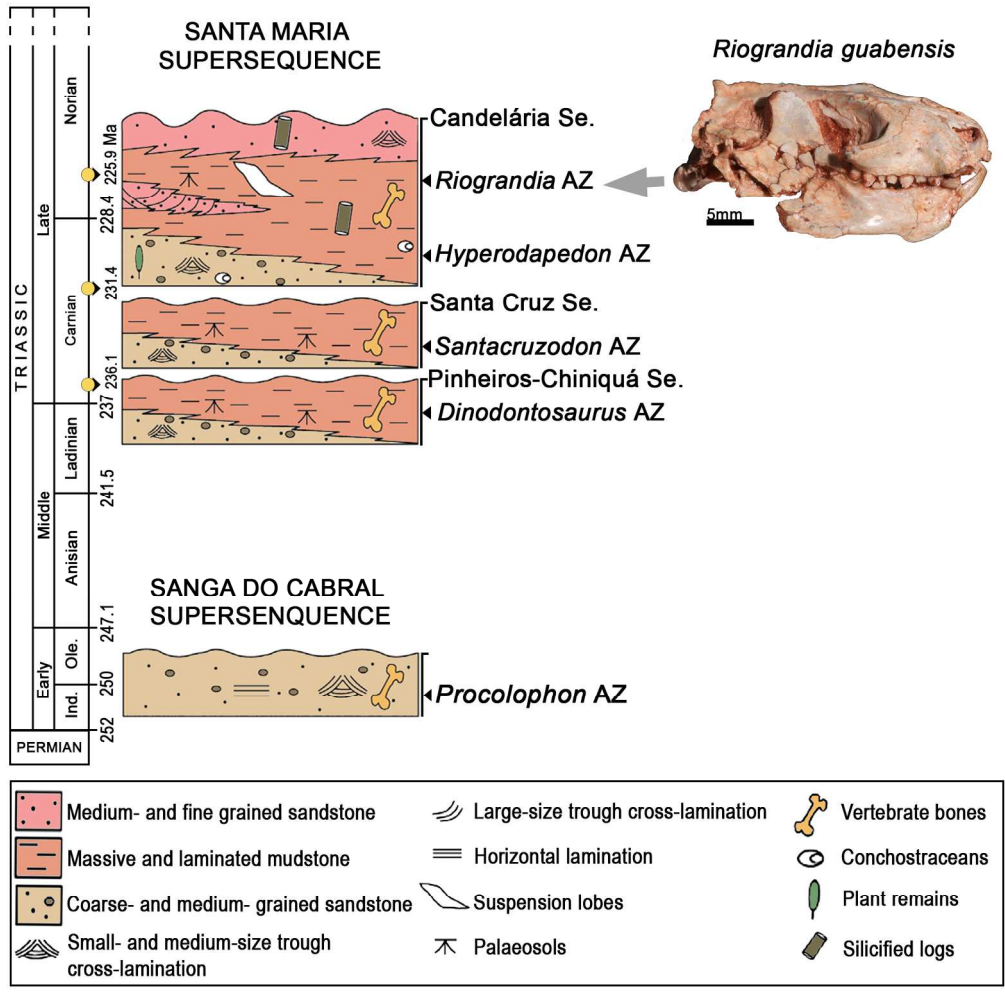


Figure 1 - Chronostratigraphy of the Triassic of Southern Brazil with vertebrate biozones (modified from Horn et al. 2014).

179x178mm (300 x 300 DPI)

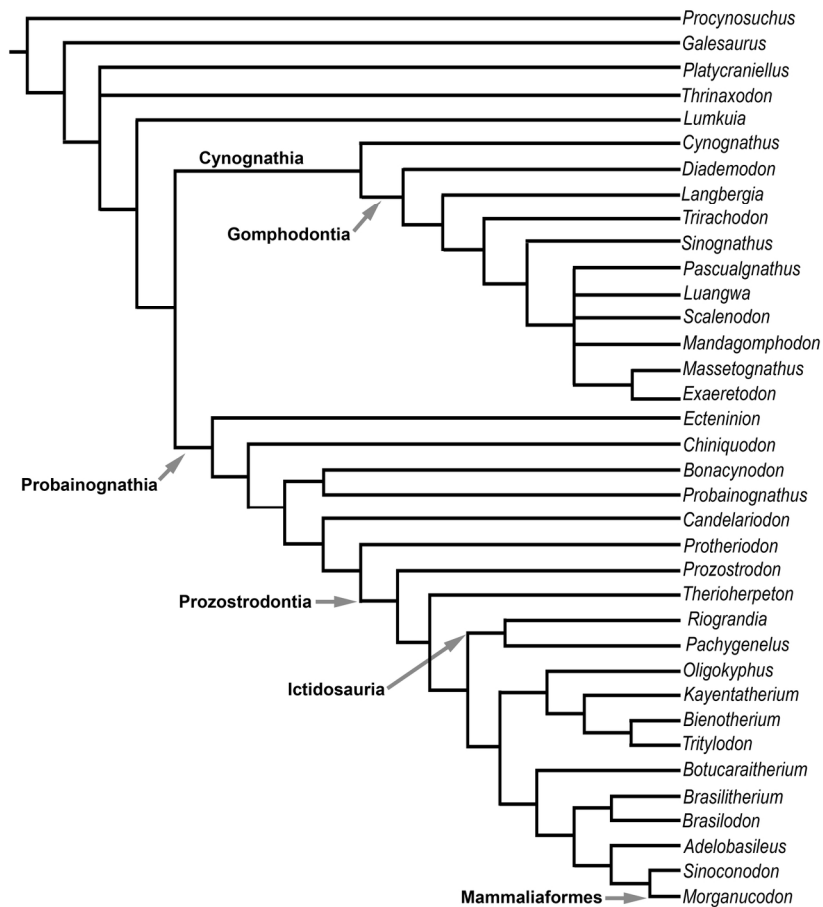


Figure 2 - Cladogram showing phylogenetic relationship among cynodont taxa, including Mammalia, according to the analysis of Martinelli et al. (in press).

166x152mm (300 x 300 DPI)

1  
2  
3  
4  
5  
6  
7  
8  
9  
10  
11  
12  
13  
14  
15  
16  
17  
18  
19  
20  
21  
22  
23  
24  
25  
26  
27  
28  
29  
30  
31  
32  
33  
34  
35  
36  
37  
38  
39  
40  
41  
42  
43  
44  
45  
46  
47  
48  
49  
50  
51  
52  
53  
54  
55  
56  
57  
58  
59  
60

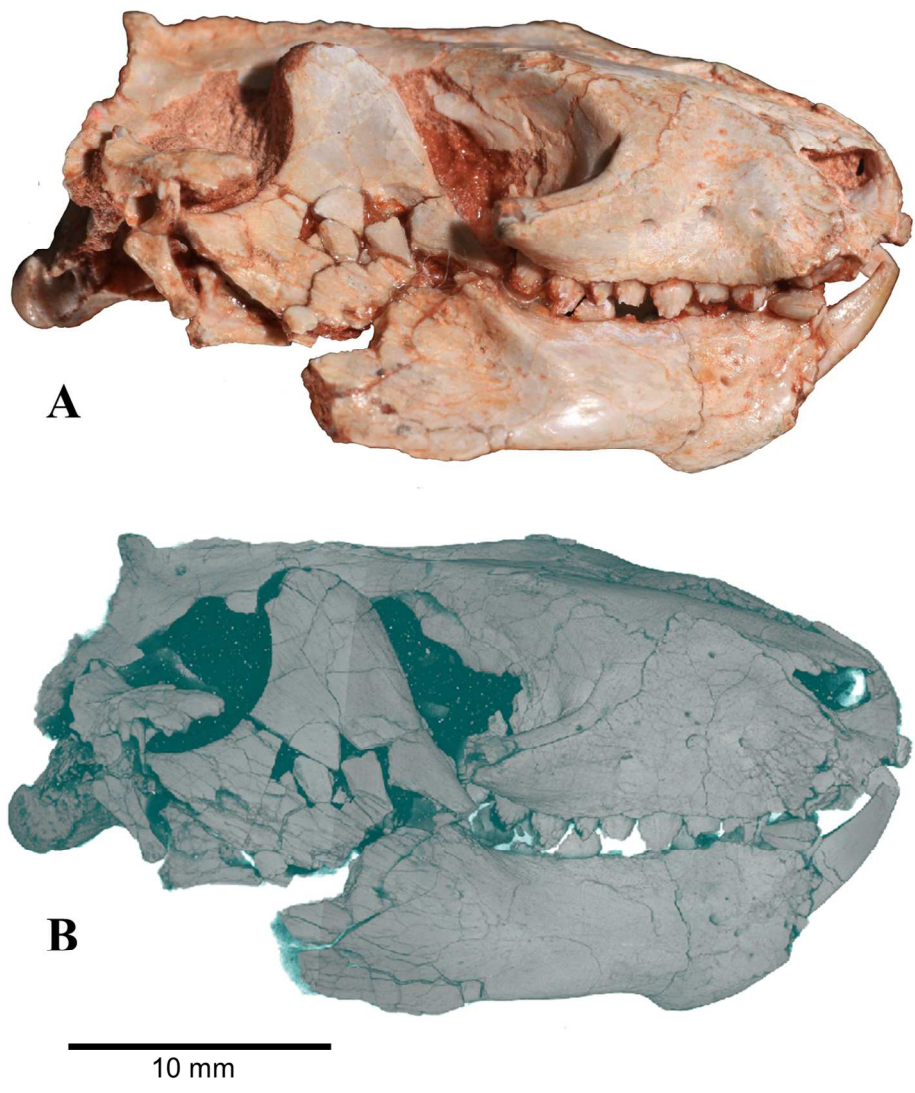


Figure 3 – The specimen *Riograndia guaibensis* UFRGS-PV-596-T in lateral view. Photograph (A) and the 3D image from CT scan (B).

255x310mm (150 x 150 DPI)

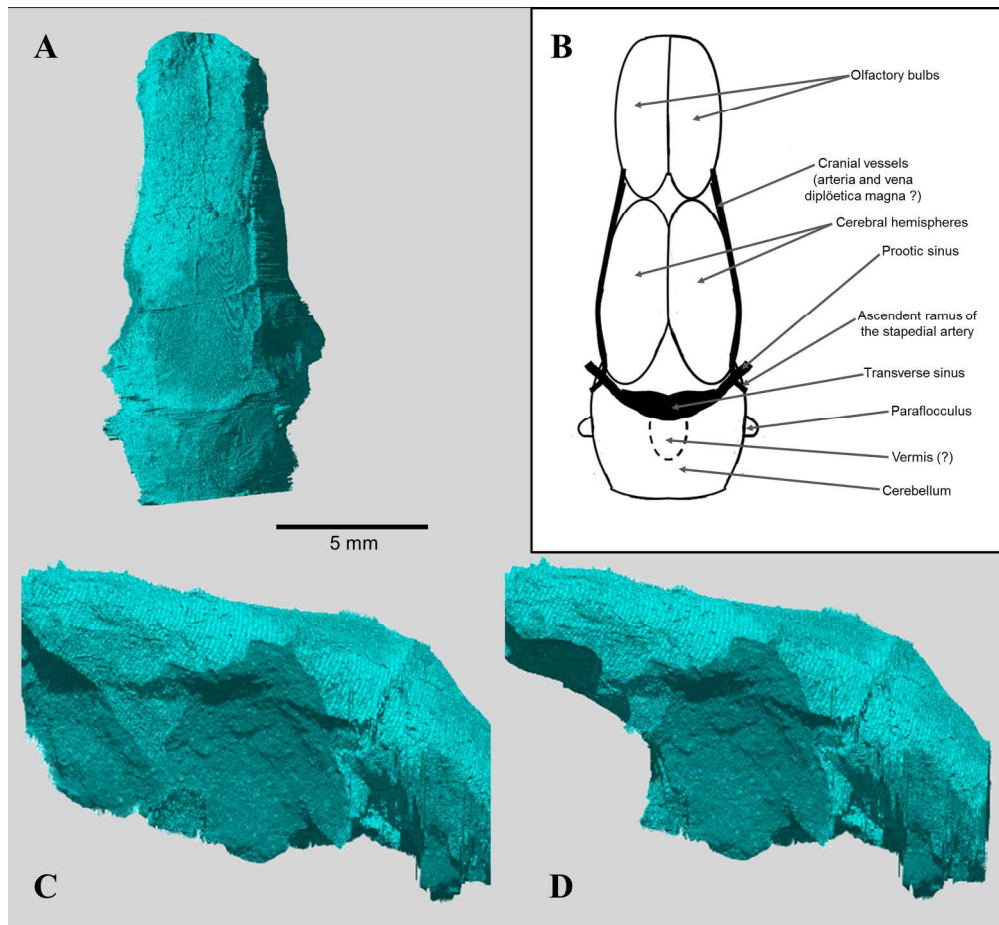


Figure 4 – Digital endocast of *Riograndia* UFRGS-PV-596-T in dorsal (A) and lateral view (C and D) and a schematic reconstruction of the dorsal view in B. with The filling of the orbital vacuity digitally removed in D.

369x340mm (150 x 150 DPI)

Only

1  
2  
3  
4  
5  
6  
7  
8  
9  
10  
11  
12  
13  
14  
15  
16  
17  
18  
19  
20  
21  
22  
23  
24  
25  
26  
27  
28  
29  
30  
31  
32  
33  
34  
35  
36  
37  
38  
39  
40  
41  
42  
43  
44  
45  
46  
47  
48  
49  
50  
51  
52  
53  
54  
55  
56  
57  
58  
59  
60

1  
2  
3  
4  
5  
6  
7  
8  
9  
10  
11  
12  
13  
14  
15  
16  
17  
18  
19  
20  
21  
22  
23  
24  
25  
26  
27  
28  
29  
30  
31  
32  
33  
34  
35  
36  
37  
38  
39  
40  
41  
42  
43  
44  
45  
46  
47  
48  
49  
50  
51  
52  
53  
54  
55  
56  
57  
58  
59  
60

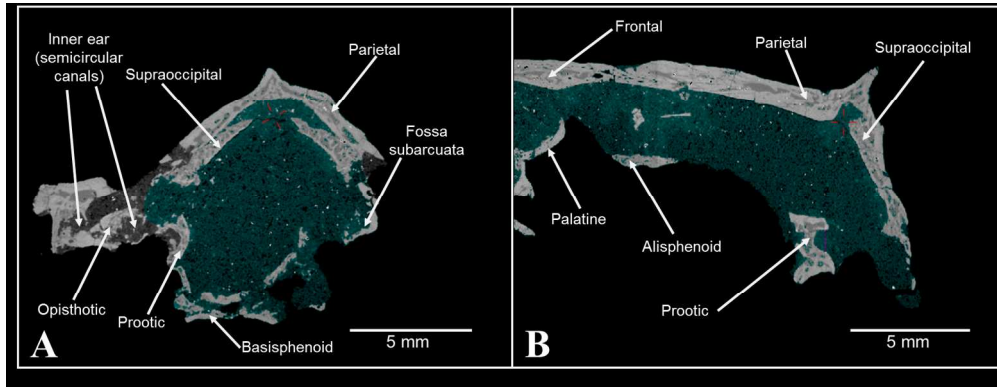


Figure 5 – Slices in coronal (A) and sagittal planes showing the unossified zone (the red mark corresponds to the same point in the two planes).

323x125mm (150 x 150 DPI)

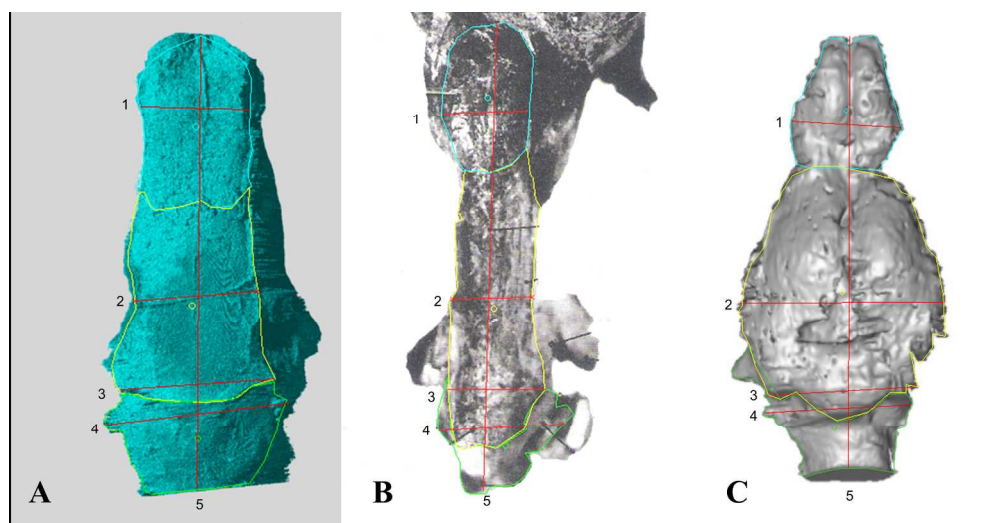
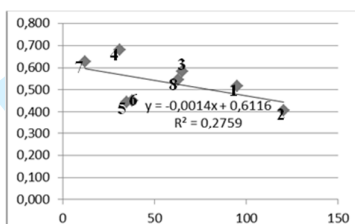


Figure 6 – Examples of the measurements taken on the dorsal surface of the endocast of *Riograndia* (A) and other taxa from images of other works, *Probelesoson* (modified from Quiroga, 1979; B) and *Vincelestes* (modified from Macrini, 2006; C): areas of the regions of olfactory bulbs region (line blue), cerebral hemispheres (line yellow), and cerebellum (line green); maximum width of the olfactory bulbs region (1), width of the cerebral hemispheres region at the half of the length (2), width of the cerebral hemispheres region near to the posterior limit (3), width of the cerebellar region (4), and the endocast length (5).

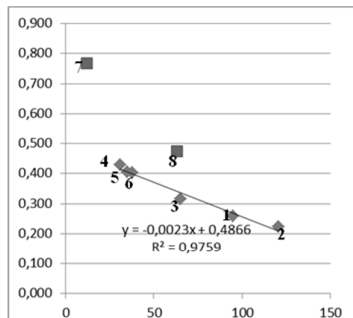
397x205mm (150 x 150 DPI)

## Appendix 1

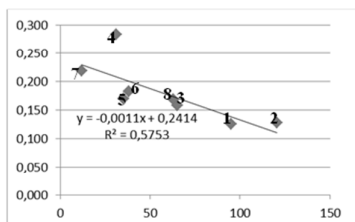
Graphics showing relationships between the ratios of the measurements of the endocast and skull for different cynodont taxa (1, *Massetoganthus*; 2, *Probelesodon*; 3, *Probainognathus*; 4, *Therioherpeton*; 5, *Riograndia*; 6, *Brasilitherium*; 7, *Hadrocodium*; 8, *Vincelestes*).



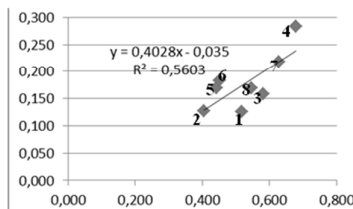
Graphic 1: Relative length of the endocast (endocast/skull) x skull length.



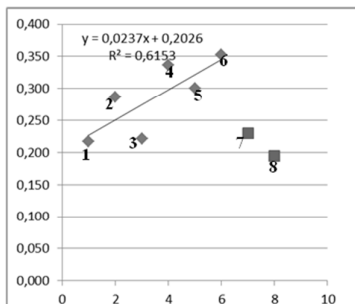
Graphic 2: Aspect ratio (maximum width/length) of the endocast x skull length (7 and 8 excluding from the trendline).



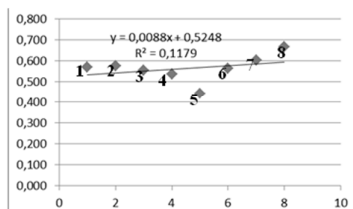
Graphic 3: Relative length of the olfactory bulbs region (olfactory bulbs/endocast) x skull length.



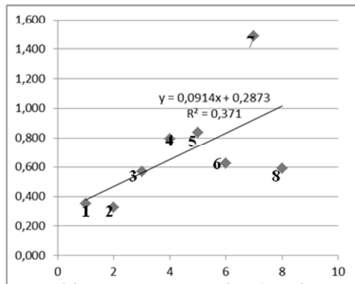
Graphic 4: Relative length of the olfactory bulbs region (olfactory bulbs/endocast) x relative length of the endocranial space (endocast/skull).



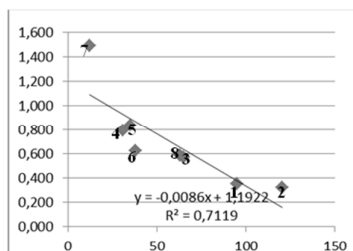
Graphic 5: Relative area of the olfactory bulbs region (olfactory bulbs/endocast) x phylogenetic proximity to mammals (7 and 8 excluding from the trendline).



Graphic 6: Aspect ratio (maximum width/length) of the cerebral hemispheres region x phylogenetic proximity to mammals.



Graphic 7: Aspect ratio (maximum width/length) of the cerebral hemispheres region x phylogenetic proximity to mammals



Graphic 8: Aspect ratio (maximum width/length) of the cerebral hemispheres region x skull length

1  
2  
3  
4  
5  
6  
7  
8  
9  
10  
11  
12  
13  
14  
15  
16  
17  
18  
19  
20  
21  
22  
23  
24  
25  
26  
27  
28  
29  
30  
31  
32  
33  
34  
35  
36  
37  
38  
39  
40  
41  
42  
43  
44  
45  
46  
47  
48  
49  
50  
51  
52  
53  
54  
55  
56  
57  
58  
59  
60

For Peer Review Only